Radiologic findings of IgG4-related disease

Yasunari Fujinaga, MD,*[1] Masumi Kadoya, MD,[1] Shigeyuki Kawa,[2] MD, Hideaki Hamano, MD,[3] Mitsuhiro Momose, MD,[1] Satoshi Kawakami, MD,[1] Tomoharu Watanabe, MD,[1] Yukiko Sugiyama, MD,[1] Takeshi Uehara, MD[4]

[1]Department of Radiology, [3]Department of Gastroenterology, Shinshu University School of Medicine, 3-1-1 Asahi, Matsumoto 390-8621, Japan.

[2]Center for Health, Safety and Environmental Management, Shinshu University, 3-1-1 Asahi, Matsumoto 390-8621, Japan.

[4]Department of Laboratory Medicine, Shinshu University School of Medicine

Correspondence should be addressed to

Yasunari Fujinaga

Department of Radiology, Shinshu University School of Medicine, 3-1-1 Asahi, Matsumoto 390-8621, Japan.

Tel: +81-263-37-2650

Fax: +81-263-37-3087

E-mail: fujinaga@shinshu-u.ac.jp

Abstract

Autoimmune pancreatitis (AIP), characterized by an autoimmune phenomenon of prominent lymphocytes, IgG4-bearing plasma cell infiltration and storiform fibrosis, has been widely reported as a specific type of chronic pancreatitis. Typical image findings of this disease are reported as diffuse pancreatic swelling and a capsule-like rim on CT or MRI. However, AIP presents with a variable morphology, such as focal, segmental and multifocal swellings. Because imaging findings for AIP can look like those of pancreatic cancer, AIP has often been treated with unnecessary surgical resection. In addition, AIP is complicated by the involvement of various other organs besides the pancreas that show lymphoplasmacytic infiltration and fibrosis. These are frequently misdiagnosed as inherent lesions of corresponding organs. Furthermore, these extra-pancreatic lesions show systemic distribution and share common features of IgG4-bearing plasma cell infiltration as well as favorable responses to corticosteroid, indicating the presence of systemic condition, IgG4-related diseases. AIP is now recognized as an IgG4-related disease. Detailed evaluations of imaging findings of CT, MRI and Gallium-67 (Ga-67) scintigraphy for the involvement of these various organs are useful for a correct diagnosis of this systemic disease.

Key words: autoimmune pancreatitis, extra-pancreatic lesion, IgG4, CT, MRI, Ga-67 scintigraphy

Introduction

Autoimmune pancreatitis (AIP), characterized by an autoimmune process, has been widely known as a specific type of chronic pancreatitis [1-14]. Its pathology was recognized as 'lymphoplasmacytic sclerosing pancreatitis' (LPSP), because prominent lymphoplasmacytic infiltration, storiform fibrosis and obstructive phlebitis were observed. Though clinical, pathologic and imaging findings of AIP were quite different from those of other pancreatic diseases [2, 15-18], AIP represents approximately 7% of patients with chronic pancreatitis [10] and 2-6% of patients who undergo pancreatic surgical resection mistakenly because the imaging findings resembled those of pancreatic cancer [19-21]. AIP should be differentiated from these diseases, especially from pancreatic cancer, because of a favorable response to corticosteroid therapy [3, 4, 6].

In addition, a variety of extra-pancreatic lesions, such as lachrymal and salivary gland lesions [22-24], hilar lymphadenopathy [24, 25], interstitial pneumonia [24, 26, 27], sclerosing cholangitis [2, 8, 24, 28-30], retroperitoneal fibrosis [12, 24, 29, 31-33], renal lesions [24, 34, 35], and prostatic lesions [24, 36-38] have been reported to be complicated with AIP. Extra-pancreatic lesions show systemic distribution and share similar pathological and clinical findings with AIP, such as storiform fibrosis, prominent lymphoplasmacytic infiltration and abundant IgG4-bearing plasma cells [12, 22, 25, 33], and have a favorable response to corticosteroid therapy [3, 4, 13-15, 22, 28-30]. Furthermore, these extra-pancreatic lesions indicated the presence of systemic condition, IgG4-related diseases [2, 12, 22, 33, 39-42]. AIP is now recognized as an IgG4-related

disease. For correct diagnosis and appropriate treatment, it is important to discriminate extra-pancreatic lesions from the inherent lesions of corresponding organs.

In this article, we report useful CT and MR findings to define AIP, and characteristic CT, MR and Ga-67 scintigraphy findings of systemic condition, IgG4-related diseases.

Radiologic findings of AIP

Early radiologic findings of AIP

In 1992, Toki et al [43] reported a case of unusual chronic pancreatitis showing diffuse irregular narrowing of the entire main pancreatic duct (MPD) on endoscopic retrograde cholecystopancreatography (ERCP) (Fig. 1). In 1995, Yoshida et al [3] proposed that this specific pancreatic disease was a form of AIP with characteristic ERP features because it was characterized by a peculiar histopathology with lymphoplasmacytic infiltration and the presence of serum immunoglobulin abnormality such as immunoglobulin G (IgG). Accordingly, early radiologic findings of AIP were analyzed mainly based on ERCP findings.

Typical CT findings of AIP

CT is a useful tool for evaluating morphologic change of the pancreas, and the hemodynamics of the pancreas are shown by dynamic contrast-enhanced CT.
In 1998, the characteristic CT features of AIP were reported by two authors [17, 18] as follows: 1) diffuse pancreatic swelling (sausage-like enlargement), 2) capsule-like rim,

3) loss of lobularity (Fig. 2).

Diffuse pancreatic swelling is caused by the involvement of abundant inflammatory cell infiltration and fibrosis. As the normal pancreas is well enhanced on the early phase of dynamic contrast-enhanced CT because of rich blood flow, decreased enhancement is found in the case of AIP, i.e., AIP is shown as low-density compared with normal pancreatic parenchyma. A capsule-like rim was obvious on contrast-enhanced CT, which is observed as a low-density area surrounding the pancreas on the early phase of dynamic contrast-enhanced CT and as a slightly high-density area on the delayed phase. The capsule-like rim is thought to be composed of dense fibrosis, which agrees with the previous result of radiologic-pathologic correlation [17]. These typical AIP findings are specific and useful for discriminating between alcoholic chronic pancreatitis and acute pancreatitis, and have been widely used. In addition, Hamano et al [11] reported that elevated serum immunoglobulin G4 (IgG4) level was a specific finding of AIP, and serum IgG4 has played a major role in diagnostic criteria [44]. To date, we have diagnosed 112 AIP patients and observed diffuse pancreatic swelling in 53.6% and a capsule-like rim in 29.5%. Other studies with large cohorts showed diffuse pancreatic swelling in 22 – 95% of patients and a capsule-like rim in 12 - 90% [45-47].

MR features of AIP

Highly contrasted pancreatic images can be obtained by magnetic resonance imaging (MRI). Normal pancreatic parenchyma has either a homogeneous or cobblestone appearance and appears as a hyperintense area on fat-suppressed

T1-weighted images (Fig. **3**). When mass lesions or inflammatory lesions are present in the pancreas, these lesions are observed as hypointense area compared with surrounding pancreatic parenchyma. So AIP is observed as a hypointense area (Fig. **4a**). On T2-weighted images and diffusion-weighted images, AIP in the active phase is observed as a homogeneous hyperintense lesion due to the involvement of inflammatory cells (Fig. **4b,c**). We need to point out that these MR findings of AIP are in many cases similar to those of pancreatic cancer. On magnetic resonance cholecyst pancreatography (MRCP), diffuse or focal narrowing of the MPD is seen without obstruction. Focal narrowing of MPD often has a skipped appearance on MRCP (Fig. **5**). In Japan, MRCP is not recommended for diagnostic procedures because the resolution level is not considered satisfactory. However, MRCP is less invasive than ERCP and offers superior visualization of overall MPD features even if MPD is obstructed on ERCP.

A capsule-like rim is observed as a hypointense rim on T1- and T2-weighted images, which reflects dense fibrosis, and the sensitivity for detecting the capsule-like rim is higher on MRI than on CT (Fig. **6**).

Gallium-67 (Ga-67) scintigraphy and F-18 fluorodeoxyglucose positron emission tomography (FDG-PET)

Ga-67 scintigraphy has been performed in whole-body surveys for inflammatory disease and malignant tumor such as malignant lymphoma. The mechanisms of Ga-67 uptake appear to involve high affinity for tumor cells or inflammatory cells that cancer invasion often induces. In AIP patients, increased uptake of Ga-67 is often seen in the

pancreas (Fig. **7**), but it is unclear how often in pancreatic cancer.

F-18 fluorodeoxyglucose (FDG) is a glucose analog that is trapped by cells with glucose transporter and phosphorylated by hexokinase. It has been used for diagnosis, staging and the evaluation of therapeutic effect, particularly in cases of malignant lymphoma, lung cancer and gynecological malignancies, in which saccharometabolism is increased. Increased uptake of FDG is also seen in pancreatic cancer and used in its diagnosis. However, increased uptake of FDG is often seen in AIP patients, because FDG is easily trapped by inflammatory cells in AIP tissue (Fig. **8**) [48-50].

In this way, Ga-67 scintigraphy and FDG-PET are useful for detecting AIP lesions but are not always useful for differentiating between AIP and pancreatic cancer [48].

Atypical findings of AIP

AIP sometimes appeared as a focal or segmental form of pancreatic lesion (Fig. **9**). In our experience of 112 AIP patients, focal or segmental swelling was observed in 23.2%, and other authors have reported 9 – 30% frequencies [45-47]. In addition, AIP with multifocal lesions has been reported [51-54] and was found in 7.1% of our cases (Fig. **10**). These focal, segmental or multifocal forms of AIP indicate that inflammation, more specifically the involvement of lymphocyte and IgG4-bearing plasma cells, was sometimes heterogeneously distributed.

Calcification was rare in AIP though common in alcoholic chronic pancreatitis. However, it was sometimes seen in cases with repeating relapse, and CT findings mimicked those of chronic alcoholic pancreatitis (Fig. **11**) [55, 56].

Cyst formation and peripancreatic strandings such as acute pancreatitis are rarely found in AIP patients. Rapid resolution of cysts was observed in AIP cases after corticosteroid therapy (Fig. **12**)[57-59].

Differentiation between focal AIP and pancreatic cancer

Focal AIP has often been misdiagnosed as pancreatic cancer, and 2 – 6% of AIP patients have received an unnecessary pancreatic surgical resection [19-21]. It is very important to differentiate between focal AIP and pancreatic cancer by noninvasive diagnostic imaging before therapy. Previously cited typical findings of AIP and findings of MPD penetrating through the mass lesion (duct-penetrating sign) on MRCP are helpful for discrimination [60], but its sensitivity is relatively low. Wakabayashi et al [61] reported that homogeneity on the delayed phase of dynamic contrast-enhanced CT was a useful finding for discrimination in a small cohort (Fig. **13**), though most cases of pancreatic cancer were observed as heterogeneous lesions (Fig. **14**). Because MRI has superior tissue contrast to CT, we analyzed the MR signal patterns in focal AIPs and found that AIP characteristics include speckled hyperintensity on precontrast and arterial-dominant phase contrast-enhanced fat-suppressed T1-weighted images, as well as homogeneous iso- or hypointensity on the equilibrium phase [62] (Fig. **15**). Residual hyperintense areas may correspond to residual pancreatic parenchyma because residual pancreatic lobules were frequently found in AIP pathologically [63]. When a differential diagnosis is difficult, indirect findings of focal AIP, such as extra-pancreatic lesions, might be helpful in addition to direct findings [24]. It goes without saying that a biopsy

is needed if definite diagnosis remains elusive.

Extra-pancreatic lesions associated with AIP and IgG4-related diseases

Many authors have reported extra-pancreatic lesions associated with AIP, such as lachrymal and salivary [22, 64], lung [26, 27, 65-68], mediastinal [25], bile duct [8, 28, 69], renal [34, 35, 70, 71], retroperitoneal [12] and prostatic [36-38] lesions. Recently, the concept of 'IgG4-related diseases' has been proposed because pathological findings similar to those of pancreatic lesion, more specifically infiltration of IgG4-bearing plasma cells, lymphocyte and fibrosis, were found in these extra-pancreatic lesions [2, 12, 22, 33, 39-42]. To detect these lesions, Ga-67 scintigraphy and FDG-PET are useful, because it is unrealistic to perform whole-body screening by CT or MRI. We described each lesion in detail, followed by case presentations of 2 AIP patients with various extra-pancreatic lesions or IgG4-related diseases.

Case presentation 1

A 50-year-old man who complained of epigastralgia and dull back pain was referred to our hospital. He had been diagnosed with Sjögren's syndrome 10 years earlier and had been followed up at another hospital. An abdominal ultrasound revealed a hypoechoic mass in the pancreas body (Fig. **16a**). A curved coronal image that was reconstructed from the early phase of dynamic contrast-enhanced CT showed a slightly low-density area in the pancreas body and mild dilatation of the main pancreatic duct (Fig. **16b**). On a CT image from another slice, bronchial thickening of the lung (Fig.

16c) and hilar lymphadenopathy (Fig. **16d**) were seen. On reconstructed coronal contrast-enhanced CT, mass lesions of bilateral renal hilum (Fig. **16e**), paravertebral mass lesion (Fig. **16e**), parasacral mass lesion (Fig. **16e**), and an orbital mass lesion (Fig. **16f**) were observed. Ga-67 scintigraphy demonstrated an increased uptake in these regions. At first, the pancreatic lesion was suspected to be pancreatic cancer. However, the full spectrum of image findings suggested a diagnosis of focal AIP with AIP-associated extra-pancreatic lesions, which was further supported by a markedly elevated serum IgG4 level (1200 mg/dl). After corticosteroid therapy, the accumulation of Ga-67 disappeared in each lesion.

This case demonstrated that AIP and multiple AIP-associated extra-pancreatic lesions may occur simultaneously. This result suggests that, upon discovering a pancreatic lesion, it is important to thoroughly examine all other organs.

Case presentation 2

A 69-year-old man exhibited obstructive jaundice and was treated with endoscopic nasobiliary drainage. An early phase of dynamic contrast-enhanced CT revealed marked thickening of the common bile duct wall but no pancreatic swelling (Fig. **17a**). On coronal contrast-enhanced CT, a para-aortic soft tissue density was found (Fig. **17b**), and Ga-67 scintigraphy demonstrated increased hilar uptake. These were suspected to be AIP-associated extra-pancreatic lesions. However, there were no abnormal findings in the pancreas. Because IgG4-bearing plasma cells were found in a biopsy specimen from the common bile duct, corticosteroid therapy was administered.

After therapy, the lesions improved and the corticosteroid dosage was tapered off. Thirty-four months after therapy, the bile duct lesion relapsed, and a new pancreatic lesion showing swelling and a capsule-like rim, which was consistent with AIP, was prominent (Fig. **17c**).

This case suggested that AIP and AIP-associated extra-pancreatic lesions may not always occur synchronously. Therefore, successive diagnostic imaging is mandatory for the correct diagnosis of newly occurring lesions.

Lachrymal and salivary gland lesions

Ga-67 scintigraphy detected lachrymal or salivary gland lesions in 47.5% of AIP patients [24]. Ga-67 scintigraphy is sensitive because it shows increased uptake in either the lachrymal or salivary gland in 95% of patients who showed clinical symptoms and were diagnosed by biopsy (Fig. **18a**) [24]. Among lachrymal or salivary gland lesions, those of the submandibular and lachrymal glands are more common than those of the parotid gland and sublingual lesions. These lesions appear symmetrically in most patients. MRI shows a bilateral homogeneous swelling of the glands without a discernable mass (Fig. **18b, c**), but shows normal findings in many patients with AIP-associated lesions.

Common differential diagnoses of salivary and lachrymal gland swelling are Sjögren's syndrome, Mikulicz disease, and Küttner tumors. Recent reports have shown that high serum IgG4 concentrations and abundant IgG4-bearing plasma cell infiltration were associated with Mikulicz disease and Küttner tumors, but not Sjögren's syndrome,

and the lachrymal or salivary gland lesions associated with AIP are considered to be in a similar condition to those in Mikulicz disease and Küttner tumors [40, 72-74]. CT and MRI frequently show lachrymal and/or submandibular swelling in AIP-associated lesions, whereas they frequently show parotid gland swelling in Sjögren's syndrome. Ga scintigraphy is useful for lesion detection, and neck MRI is useful for differential diagnosis between AIP-associated lesions and Sjögren's syndrome because the salt-and-pepper appearance characteristic of MR findings in Sjögren's syndrome is not seen in AIP-associated lesions [75].

Hilar lymphadenopathy

Hilar lymphadenopathy is one of the most common lesions associated with AIP and is detected by contrast-enhanced CT or Ga-67 scintigraphy (Fig. **19**) [24, 25, 76]. High-resolution CT, less than 3 mm slice thickness, will improve the visualization of bilateral hilar lymphadenopathy. Careful examination is needed for the assessment of Ga-67 scintigraphy because physiological hilar uptake is seen in normal patients. Differential diagnosis of hilar lymphadenopathy includes sarcoidosis and primary biliary cirrhosis. In AIP-associated lesions, hilar lymphadenopathy and systemic Ga-67 accumulation are often found and helpful for making a diagnosis. In addition, elevated serum IgG4 value, increased IgG4 in the bronchoalveolar lavage and a normal serum ACE value might be helpful for the exclusion of sarcoidosis [68].

Pulmonary abnormalities

High-resolution thoracic CT revealed lung lesions in 54% of AIP patients [24]. There are various types of lesions, such as nodular lesions, bronchial thickening, interlobular thickening, and consolidation (Fig. **20**) [24]. Nodular lesions and bronchial thickening are most prevalent. Inoue et al [66] reported on IgG4-related lung lesions with pathological correlations and mentioned that various radiologic findings, such as ground-glass opacity, thickening of bronchovascular bundle and interlobular septa, bronchioectasia, and nodular lesion, correspond to IgG4-related sclerosing inflammation along the intrapulmonary connective tissue. In this report, AIP was identified in only 3 of 13 patients; thus, there are various IgG4-related lesions without relation to AIP.

Radiologically, the differential diagnosis of nodular lesions associated with AIP includes nonspecific inflammatory nodules, lung cancer, Wegener's granulomatosis and Castleman's lymphoma. Differential diagnosis of other types of AIP-related or IgG4-related lung lesions, which appear in interstitial spaces containing lymphoid channels, includes chronic bronchitis, chronic bronchiolitis, nonspecific interstitial pneumonia (NSIP), and lymphocytic interstitial pneumonia (LIP). For discrimination, it is useful to find pancreatic and other extra-pancreatic lesions as well as to check serum IgG4 levels.

Bile duct abnormalities

Bile duct abnormalities are the most common abdominal findings associated with AIP; CT or MRI showed extra-pancreatic bile duct lesions in 78% of AIP patients [24].

Extensive wall thickening with occlusion of the intrahepatic bile duct was seen in 28% of these patients, and such thickening with occlusion of the common hepatic or intra-pancreatic common bile duct was seen in 46% [24]. When the pancreas head is not swelled, bile duct dilatation is mild regardless of the wall thickening. MRI is a useful tool for evaluating these lesions (Fig. **21**), and some cases show prominent wall thickening with a laminar structure and focal wall thickening of the common bile duct. MRCP sometimes shows intrahepatic bile duct narrowing, which mimics primary sclerosing cholangitis (PSC). When pancreatic head swelling is prominent, severe bile duct dilatation occurs.

The differential diagnosis of bile duct abnormality associated with AIP includes PSC and biliary malignancies. Characteristic findings of ERCP were reported as a band-like stricture, a beaded appearance, a pruned-tree appearance, and diverticulum-like outpouching [77-79]. However, it is sometimes difficult to differentiate between AIP- and PSC-related lesions. We need to search for pancreatic and extra-pancreatic lesions, to elucidate their etiology, and to assess their response to corticosteroid therapy. Bile duct carcinoma typically shows severe bile duct dilatation with focal wall thickening or mass lesion, though AIP-associated lesions show mild duct dilatation with extensive wall thickening. However, it should be kept in mind that severe bile duct dilatation may occur when pancreas head swelling is prominent in AIP. And when it is difficult to discriminate AIP-related bile duct lesions from bile duct carcinoma, we recommend biopsy.

Peri-pancreatic and para-aortic lymphadenopathy

Peri-pancreatic or para-aortic lymphadenopathy was seen in 57% of AIP cases (Fig. **22**) [24]. CT or MRI clearly demonstrates these lesions, but it is often difficult to differentiate AIP-related lymphadenopathy from others, such as nonspecific inflammatory lymph node swelling, multicentric Castleman's disease and malignant lymphoma.

Renal lesions

Renal lesions were seen in 14-30% of AIP patients, including parenchymal lesions, hilar lesions and perirenal lesions (Fig. **23**) [24, 80]. Parenchymal lesions are the most common subtype of renal lesions, and correspond to tubulointerstitial nephritis with lymphoplasmacytic infiltration and fibrosis [34]. Dynamic contrast-enhanced CT or MRI shows poorly enhanced multiple wedge-shaped or round lesions of bilateral kidney in the arterial dominant phase and ill-defined lesions in the delayed phase [80]. In addition, CT sometimes shows renal swelling [34, 35], and it is one of the important finding of renal lesions. It is hard to detect these lesions on T1-weighted images, but T2-weighted and diffusion-weighted images reveal them as hyperintense lesions. Pyelonephritis and renal infarctions sometimes mimic radiological findings, and clinical manifestations are helpful for differential diagnosis. On CT or MRI, pelvic lesions and perirenal lesions are seen as prominent and diffuse renal pelvic wall thickening in renal hilus and perirenal mass-like lesions, respectively (Fig **23b**, **c**). To find complicating pancreatic and extra-pancreatic lesions would give suggestions that the renal lesions are

not ureteral tumor nor malignant lymphoma but IgG4-related lesions.

Retroperitoneal lesions

Retroperitoneal lesions are observed in 9.1-20% of AIP patients and include four types: periaortic, periureteric, parabone and increased fat density types (Fig. **24**) [24, 81]. The periaortic type is seen as soft tissue masses around the aorta and sometimes causess periaortitis or aortic aneurysm. The periureteric type consists of soft tissue masses around both ureters and may cause hydronephrosis. The parabone type appears as soft tissue masses in contact with vertebrae, parailiac bone or sacral bone, and is asymptomatic. The increased fat density type appears as increased attenuation around the superior mesenteric artery or celiac artery mimicking mesenteric panniculitis.

Other lesions

Other rare extra-pancreatic lesions such as hypophysitis (Fig. **25**) [82], prostatic lesions (Fig. **26**) [24], pericardial lesions (Fig. **27**) [83] and *ligamentum teres* lesions (Fig. **28**) [24] were reported. IgG4-related hypophysitis manifests as pituitary gland or stalk swelling and will improve after corticosteroid therapy. Prostatic lesions correspond to prostatic hyperplasia and are indicated by an enlarged prostate, abnormal accumulation on Ga-67 scintigraphy and hyperintensity on diffusion-weighted images. Pericardial and *ligamentum teres* lesions represent as pericardial and *ligamentum teres* soft tissue masses, respectively. In addition, we experienced asymptomatic infraorbital nerve swelling associated with AIP (Fig. **16f**). Though the mechanisms or etiologies of

these lesions are unknown, they respond well to corticosteroid therapy.

Extra-pancreatic lesions without pancreatic lesions

As presented in case 2, pancreatic lesions are sometimes absent when extra-pancreatic lesions are found by diagnostic imaging. In 1978, Nakano et al reported a case with a vanishing tumor in the abdomen followed by Sjögren's syndrome, and this case showed a favorable response to corticosteroid therapy. That report seems to be the first to document IgG4-related systemic disease with improvement by corticosteroid therapy. We experienced some patients who suffered from IgG4-related extra-pancreatic lesions, such as sialadenitis, lung lesion, hilar lymphadenopathy, liver lesions, sclerosing cholangitis, renal lesions, retroperitoneal lesions and prostatic lesions, without pancreatic lesions (Fig. **29**). In most cases, all of the extra-pancreatic lesions were detectable by radiologic imaging. These lesions are now included in IgG4-related diseases.

In most reports that described patients having IgG4-related extra-pancreatic lesions without pancreatic lesions, whole body surveys by diagnostic imaging were not performed. Therefore, the exact frequency and prevalence are unknown, and it is unclear when and whether these imaging tests can detect AIP. Ga-67 scintigraphy and FDG-PET are useful methods for whole body survey and the assessment of therapeutic effects.

Conclusion

It is easy to diagnose AIP when typical AIP findings are found in radiologic imaging. On the other hand, it is important to analyze radiologic findings in detail in order to differentiate AIP from alcoholic chronic pancreatitis and pancreatic cancer by using characteristic AIP findings, such as the homogeneity of pancreatic lesions on delayed-phase dynamic contrast-enhanced CT or MRI, and speckled hyperintensity on precontrast or arterial dominant-phase dynamic contrast-enhanced fat-suppressed T1-weighted images. The presence of extra-pancreatic lesions is helpful for diagnosing AIP, but a detailed evaluation of radiologic images is needed in order to discriminate AIP-related extra-pancreatic lesions from the inherent lesions of corresponding organs. Furthermore, we should recognize the wide spectrum of systemic lesions as IgG4-related diseases.

References

[1] Sarles H, Sarles JC, Muratore R, Guien C. Chronic inflammatory sclerosis of the pancreas--an autonomous pancreatic disease? Am J Dig Dis 1961;6:688-98.

[2] Kawaguchi K, Koike M, Tsuruta K, Okamoto A, Tabata I, Fujita N. Lymphoplasmacytic sclerosing pancreatitis with cholangitis: a variant of primary sclerosing cholangitis extensively involving pancreas. Hum Pathol 1991;22(4):387-95.

[3] Yoshida K, Toki F, Takeuchi T, Watanabe S, Shiratori K, Hayashi N. Chronic pancreatitis caused by an autoimmune abnormality. Proposal of the concept of autoimmune pancreatitis. Dig Dis Sci 1995;40(7):1561-8.

[4] Ito T, Nakano I, Koyanagi S, *et al.* Autoimmune pancreatitis as a new clinical entity. Three cases of autoimmune pancreatitis with effective steroid therapy. Dig Dis Sci 1997;42(7):1458-68.

[5] Wakabayashi T, Motoo Y, Kojima Y, Makino H, Sawabu N. Chronic pancreatitis with diffuse irregular narrowing of the main pancreatic duct. Dig Dis Sci 1998;43(11):2415-25.

[6] Horiuchi A, Kaneko T, Yamamura N, *et al.* Autoimmune chronic pancreatitis simulating pancreatic lymphoma. Am J Gastroenterol 1996;91(12):2607-9.

[7] Horiuchi A, Kawa S, Akamatsu T, *et al.* Characteristic pancreatic duct appearance in autoimmune chronic pancreatitis: a case report and review of the Japanese literature. Am J Gastroenterol 1998;93(2):260-3.

[8] Erkelens GW, Vleggaar FP, Lesterhuis W, van Buuren HR, van der Werf SD. Sclerosing pancreato-cholangitis responsive to steroid therapy. Lancet 1999;354(9172):43-4.

[9] Okazaki K, Uchida K, Ohana M, *et al.* Autoimmune-related pancreatitis is associated with autoantibodies and a Th1/Th2-type cellular immune response. Gastroenterology 2000;118(3):573-81.

[10] Uchida K, Okazaki K, Konishi Y, *et al.* Clinical analysis of autoimmune-related pancreatitis. Am J Gastroenterol 2000;95(10):2788-94.

[11] Hamano H, Kawa S, Horiuchi A, *et al.* High serum IgG4 concentrations in patients with sclerosing pancreatitis. N Engl J Med 2001;344(10):732-8.

[12] Hamano H, Kawa S, Ochi Y, *et al.* Hydronephrosis associated with retroperitoneal fibrosis and sclerosing pancreatitis. Lancet 2002;359(9315):1403-4.

[13] Kawa S, Ota M, Yoshizawa K, *et al.* HLA DRB10405-DQB10401 haplotype is associated with autoimmune pancreatitis in the Japanese population. Gastroenterology 2002;122(5):1264-9.

[14] Horiuchi A, Kawa S, Hamano H, Hayama M, Ota H, Kiyosawa K. ERCP features in 27 patients with autoimmune pancreatitis. Gastrointest Endosc 2002;55(4):494-9.

[15] Notohara K, Burgart LJ, Yadav D, Chari S, Smyrk TC. Idiopathic chronic pancreatitis with periductal lymphoplasmacytic infiltration: clinicopathologic features of 35 cases. Am J Surg Pathol 2003;27(8):1119-27.

[16] Klimstra DS, Adsay NV. Lymphoplasmacytic sclerosing (autoimmune) pancreatitis. Semin Diagn Pathol 2004;21(4):237-46.

[17] Irie H, Honda H, Baba S, *et al.* Autoimmune pancreatitis: CT and MR characteristics. AJR Am J Roentgenol 1998;170(5):1323-7.

[18] Furukawa N, Muranaka T, Yasumori K, Matsubayashi R, Hayashida K, Arita Y. Autoimmune pancreatitis: radiologic findings in three histologically proven cases. J Comput Assist Tomogr 1998;22(6):880-3.

[19] Hardacre JM, Iacobuzio-Donahue CA, Sohn TA, *et al.* Results of pancreaticoduodenectomy for lymphoplasmacytic sclerosing pancreatitis. Ann Surg 2003;237(6):853-8; discussion 8-9.

[20] Yadav D, Notahara K, Smyrk TC, *et al.* Idiopathic tumefactive chronic

pancreatitis: clinical profile, histology, and natural history after resection. Clin Gastroenterol Hepatol 2003;1(2):129-35.

[21] Abraham SC, Cruz-Correa M, Argani P, Furth EE, Hruban RH, Boitnott JK. Lymphoplasmacytic chronic cholecystitis and biliary tract disease in patients with lymphoplasmacytic sclerosing pancreatitis. Am J Surg Pathol 2003;27(4):441-51.

[22] Kamisawa T, Funata N, Hayashi Y, *et al.* Close relationship between autoimmune pancreatitis and multifocal fibrosclerosis. Gut 2003;52(5):683-7.

[23] Nakano S, Takeda I, Kitamura K, Watahiki H, Iinuma Y, Takenaka M. Vanishing tumor of the abdomen in patient with Sjögren's syndrome. Am J Dig Dis 1978;23(Suppl):75S - 9S.

[24] Fujinaga Y, Kadoya M, Kawa S, *et al.* Characteristic findings in images of extra-pancreatic lesions associated with autoimmune pancreatitis. Eur J Radiol 2009.

[25] Saegusa H, Momose M, Kawa S, *et al.* Hilar and Pancreatic Gallium-67 Accumulation is Characteristic Feature of Autoimmune Pancreatitis. Pancreas 2003;27(1):20-5.

[26] Taniguchi T, Ko M, Seko S, *et al.* Interstitial pneumonia associated with autoimmune pancreatitis. Gut 2004;53(5):770; author reply -1.

[27] Hirano K, Kawabe T, Komatsu Y, *et al.* High-rate pulmonary involvement in autoimmune pancreatitis. Intern Med J 2006;36(1):58-61.

[28] Nakazawa T, Ohara H, Yamada T, *et al.* Atypical primary sclerosing cholangitis cases associated with unusual pancreatitis. Hepatogastroenterology 2001;48(39):625-30.

[29] Hirano K, Shiratori Y, Komatsu Y, *et al.* Involvement of the biliary system in autoimmune pancreatitis: a follow-up study. Clin Gastroenterol Hepatol 2003;1(6):453-64.

[30] Horiuchi A, Kawa S, Hamano H, Ochi Y, Kiyosawa K. Sclerosing pancreato-cholangitis responsive to corticosteroid therapy: report of 2 case reports and review. Gastrointest Endosc 2001;53(4):518-22.

[31] Uchida K, Okazaki K, Asada M, *et al.* Case of chronic pancreatitis involving an autoimmune mechanism that extended to retroperitoneal fibrosis. Pancreas 2003;26(1):92-4.

[32] Fukukura Y, Fujiyoshi F, Nakamura F, Hamada H, Nakajo M. Autoimmune pancreatitis associated with idiopathic retroperitoneal fibrosis. AJR Am J Roentgenol 2003;181(4):993-5.

[33] Kamisawa T, Nakajima H, Egawa N, Funata N, Tsuruta K, Okamoto A. IgG4-related sclerosing disease incorporating sclerosing pancreatitis, cholangitis, sialadenitis and retroperitoneal fibrosis with lymphadenopathy. Pancreatology 2006;6(1-2):132-7.

[34] Takeda S, Haratake J, Kasai T, Takaeda C, Takazakura E. IgG4-associated idiopathic tubulointerstitial nephritis complicating autoimmune pancreatitis. Nephrol Dial Transplant 2004;19(2):474-6.

[35] Uchiyama-Tanaka Y, Mori Y, Kimura T, *et al.* Acute tubulointerstitial nephritis associated with autoimmune-related pancreatitis. Am J Kidney Dis 2004;43(3):e18-25.

[36] Yoshimura Y, Takeda S, Ieki Y, Takazakura E, Koizumi H, Takagawa K. IgG4-associated prostatitis complicating autoimmune pancreatitis. Intern Med 2006;45(15):897-901.

[37] Nishimori I, Kohsaki T, Onishi S, *et al.* IgG4-related autoimmune prostatitis: two cases with or without autoimmune pancreatitis. Intern Med 2007;46(24):1983-9.

[38] Uehara T, Hamano H, Kawakami M, *et al.* Autoimmune pancreatitis-associated prostatitis: distinct clinicopathological entity. Pathol Int 2008;58(2):118-25.

[39] Masaki Y, Dong L, Kurose N, *et al.* Proposal for a new clinical entity, IgG4-positive multi-organ lymphoproliferative syndrome: Analysis of 64 cases of IgG4-related disorders. Ann Rheum Dis 2008.

[40] Yamamoto M, Takahashi H, Ohara M, *et al.* A new conceptualization for Mikulicz's disease as an IgG4-related plasmacytic disease. Mod Rheumatol 2006;16(6):335-40.

[41] van der Vliet HJ, Perenboom RM. Multiple pseudotumors in IgG4-associated multifocal systemic fibrosis. Ann Intern Med 2004;141(11):896-7.

[42] Neild GH, Rodriguez-Justo M, Wall C, Connolly JO. Hyper-IgG4 disease: report and characterisation of a new disease. BMC Med 2006;4:23.

[43] Toki F, Kozu T, Oi I, Nakasato T, Suzuki M, Hanyu F. An unusual type of chronic pancreatitis showing diffuse irregular narrowing of the entire main pancreatic duct on ERCP—a report of four cases [abstract]. Endoscopy 1992;24:640.

[44] Okazaki K, Kawa S, Kamisawa T, *et al.* Clinical diagnostic criteria of autoimmune pancreatitis: revised proposal. J Gastroenterol 2006;41(7):626-31.

[45] Sahani DV, Kalva SP, Farrell J, *et al.* Autoimmune pancreatitis: imaging features. Radiology 2004;233(2):345-52.

[46] Yang DH, Kim KW, Kim TK, *et al.* Autoimmune pancreatitis: radiologic findings in 20 patients. Abdom Imaging 2006;31(1):94-102.

[47] Chari ST, Smyrk TC, Levy MJ, *et al.* Diagnosis of autoimmune pancreatitis: the Mayo Clinic experience. Clin Gastroenterol Hepatol 2006;4(8):1010-6; quiz 934.

[48] Higashi T, Saga T, Nakamoto Y, *et al.* Diagnosis of pancreatic cancer using fluorine-18 fluorodeoxyglucose positron emission tomography (FDG PET) --usefulness and limitations in "clinical reality". Ann Nucl Med 2003;17(4):261-79.

[49] Nakamoto Y, Saga T, Ishimori T, *et al.* FDG-PET of autoimmune-related pancreatitis: preliminary results. Eur J Nucl Med 2000;27(12):1835-8.

[50] Ozaki Y, Oguchi K, Hamano H, *et al.* Differentiation of autoimmune pancreatitis from suspected pancreatic cancer by fluorine-18 fluorodeoxyglucose positron emission tomography. J Gastroenterol 2008;43(2):144-51.

[51] Inoue D, Gabata T, Matsui O, Zen Y, Minato H. Autoimmune pancreatitis with multifocal mass lesions. Radiat Med 2006;24(8):587-91.

[52] Mikami K, Itoh H. MR imaging of multifocal autoimmune pancreatitis in the pancreatic head and tail: a case report. Magn Reson Med Sci 2002;1(1):54-8.

[53] Kajiwara M, Kojima M, Konishi M, *et al.* Autoimmune pancreatitis with multifocal lesions. J Hepatobiliary Pancreat Surg 2008;15(4):449-52.

[54] Fujinaga Y, Kadoya M, Ueda K, *et al.* Autoimmune pancreatitis with multifocal mass-like lesions. Eur Radiol 2009;19(Supplement 1):S348.

[55] Takayama M, Hamano H, Ochi Y, *et al.* Recurrent attacks of autoimmune pancreatitis result in pancreatic stone formation. Am J Gastroenterol 2004;99(5):932-7.

[56] Nakazawa T, Ohara H, Sano H, *et al.* Difficulty in diagnosing autoimmune pancreatitis by imaging findings. Gastrointest Endosc 2007;65(1):99-108.

[57] Nishimura T, Masaoka T, Suzuki H, Aiura K, Nagata H, Ishii H. Autoimmune pancreatitis with pseudocysts. J Gastroenterol 2004;39(10):1005-10.

[58] Welsch T, Kleeff J, Esposito I, Buchler MW, Friess H. Autoimmune pancreatitis associated with a large pancreatic pseudocyst. World J Gastroenterol 2006;12(36):5904-6.

[59] Muraki T, Hamano H, Ochi Y, *et al.* Corticosteroid-responsive pancreatic cyst found in autoimmune pancreatitis. J Gastroenterol 2005;40(7):761-6.

[60] Ichikawa T, Sou H, Araki T, *et al.* Duct-penetrating sign at MRCP: usefulness

for differentiating inflammatory pancreatic mass from pancreatic carcinomas. Radiology 2001;221(1):107-16.

[61] Wakabayashi T, Kawaura Y, Satomura Y, *et al.* Clinical and imaging features of autoimmune pancreatitis with focal pancreatic swelling or mass formation: comparison with so-called tumor-forming pancreatitis and pancreatic carcinoma. Am J Gastroenterol 2003;98(12):2679-87.

[62] Sugiyama Y, Fujinaga Y, Kurozumi M, *et al.* Characteristic features that are useful in differentiating between focal autoimmune pancreatitis and pancreatic cancer. Eur Radiol 2009;19(Supplement 1):S346-S7.

[63] Chandan VS, Iacobuzio-Donahue C, Abraham SC. Patchy distribution of pathologic abnormalities in autoimmune pancreatitis: implications for preoperative diagnosis. Am J Surg Pathol 2008;32(12):1762-9.

[64] Nakano S, Takeda I, Kitamura K, Watahiki H, Iimura Y, Takenaka M. Vanishing tumor of the abdomen in patient with Sjoegren's syndrome. Digestive Disease 1978;23:75-9.

[65] Zen Y, Kitagawa S, Minato H, *et al.* IgG4-positive plasma cells in inflammatory pseudotumor (plasma cell granuloma) of the lung. Hum Pathol 2005;36(7):710-7.

[66] Inoue D, Zen Y, Abo H, *et al.* Immunoglobulin G4-related lung disease: CT findings with pathologic correlations. Radiology 2009;251(1):260-70.

[67] Ito M, Yasuo M, Yamamoto H, *et al.* Central airway stenosis in a patient with autoimmune pancreatitis. Eur Respir J 2009;33(3):680-3.

[68] Tsushima K, Tanabe T, Yamamoto H, *et al.* Pulmonary involvement of autoimmune pancreatitis. Eur J Clin Invest 2009;39(8):714-22.

[69] Nakazawa T, Kobayashi K, Ohara H, *et al.* Autoimmune pancreatitis associated with biliary stricture, immune thronbocytopenic purpura and lung fibrosis. Digestive Endoscopy 2004;16:262-5.

[70] Saeki T, Saito A, Hiura T, *et al.* Lymphoplasmacytic infiltration of multiple organs with immunoreactivity for IgG4: IgG4-related systemic disease. Intern Med 2006;45(3):163-7.

[71] Deshpande V, Chicano S, Finkelberg D, *et al.* Autoimmune pancreatitis: a systemic immune complex mediated disease. Am J Surg Pathol 2006;30(12):1537-45.

[72] Yamamoto M, Ohara M, Suzuki C, *et al.* Elevated IgG4 concentrations in serum of patients with Mikulicz's disease. Scand J Rheumatol 2004;33(6):432-3.

[73] Yamamoto M, Takahashi H, Sugai S, Imai K. Clinical and pathological characteristics of Mikulicz's disease (IgG4-related plasmacytic exocrinopathy). Autoimmun Rev 2005;4(4):195-200.

[74] Kitagawa S, Zen Y, Harada K, *et al.* Abundant IgG4-positive plasma cell infiltration characterizes chronic sclerosing sialadenitis (Kuttner's tumor). Am J Surg Pathol 2005;29(6):783-91.

[75] Takashima S, Takeuchi N, Morimoto S, *et al.* MR imaging of Sjogren syndrome: correlation with sialography and pathology. J Comput Assist Tomogr 1991;15(3):393-400.

[76] Hamano H, Arakura N, Muraki T, Ozaki Y, Kiyosawa K, Kawa S. Prevalence and distribution of extrapancreatic lesions complicating autoimmune pancreatitis. J Gastroenterol 2006;41(12):1197-205.

[77] Nakazawa T, Ohara H, Sano H, *et al.* Clinical differences between primary sclerosing cholangitis and sclerosing cholangitis with autoimmune pancreatitis. Pancreas 2005;30(1):20-5.

[78] Nakazawa T, Ohara H, Sano H, Ando T, Joh T. Schematic classification of sclerosing cholangitis with autoimmune pancreatitis by cholangiography. Pancreas 2006;32(2):229.

[79] Nakazawa T, Ohara H, Sano H, *et al.* Cholangiography can discriminate

sclerosing cholangitis with autoimmune pancreatitis from primary sclerosing cholangitis. Gastrointest Endosc 2004;60(6):937-44.

[80] Takahashi N, Kawashima A, Fletcher JG, Chari ST. Renal involvement in patients with autoimmune pancreatitis: CT and MR imaging findings. Radiology 2007;242(3):791-801.

[81] Kamisawa T, Egawa N, Nakajima H, Tsuruta K, Okamoto A. Extrapancreatic lesions in autoimmune pancreatitis. J Clin Gastroenterol 2005;39(10):904-7.

[82] Tanabe T, Tsushima K, Yasuo M, *et al.* IgG4-associated multifocal systemic fibrosis complicating sclerosing sialadenitis, hypophysitis, and retroperitoneal fibrosis, but lacking pancreatic involvement. Intern Med 2006;45(21):1243-7.

[83] Sugimoto T, Morita Y, Isshiki K, *et al.* Constrictive pericarditis as an emerging manifestation of hyper-IgG4 disease. Int J Cardiol 2008;130(3):e100-1.

Figure legends

Fig. (1). Typical ERCP findings of AIP in a 56-year-old man.
ERCP shows diffuse irregular narrowing of the main pancreatic duct.

Fig. (2). Typical CT findings of AIP in a 61-year-old man.
(a) Precontrast CT image shows diffuse pancreatic swelling. (b) Early phase of dynamic contrast-enhanced CT image shows loss of pancreatic lobularity and a low-density rim, called a capsule-like rim (white arrows). (c) Delayed phase of dynamic contrast-enhanced CT image shows the capsule-like rim is gradually enhanced (arrowheads).

Fig. (3). Normal pancreatic findings on fat-suppressed T1-weighted images in a 63-year-old woman.
Pancreatic parenchyma is represented as a more hyperintense area than the surrounding organs.

Fig. (4). Typical MR findings of AIP in a 61-year-old man (same case as in Fig. 2).
(a) Fat-suppressed T1-weighted image shows decreased signal intensity of pancreatic parenchyma. On fat-suppressed T2-weighted image (b) and diffusion-weighted image (c), pancreatic parenchyma is seen as a hyperintense area.

Fig. (5). Skipped main pancreatic duct narrowing of AIP in a 78-year-old woman.
MRCP shows multiple skipped narrowings of the main pancreatic duct (arrows).

Fig. (6). Capsule-like rim on CT and MRI in a 63-year-old woman.
(a) On early phase of dynamic contrast-enhanced CT, the capsule-like rim is unclear. On T1-weighted image (b) and T2-weighted image (c), the capsule-like rim is obvious (arrows).

Fig. (7). Ga-67 scintigram findings of AIP in a 68-year-old man.
Ga-67 scintigrams and referential CT images show increased uptake in the lesion of the pancreatic body.

Fig. (8). FDG-PET findings of AIP in an 82-year-old man.
FDG-PET image shows nodular uptake in the lesion of the pancreas body (arrow).

Fig. (9). Segmental AIP in a 68-year-old man.
Early phase of dynamic contrast-enhanced CT shows segmented poorly enhanced area, corresponding to segmental AIP, in the pancreas body and tail.

Fig. (10). Multifocal AIP in a 53-year-old woman.
Reconstructed curved coronal image of early phase of dynamic contrast-enhanced CT shows multiple poorly enhanced areas of the pancreas (white arrows).

Fig. (11). AIP with calcifications in a 69-year-old woman.
Precontrast CT image shows calcifications and dilated main pancreatic duct.

Fig. (12). AIP with cyst formation in a 53-year-old woman.
(a) Early phase of dynamic contrast-enhanced CT shows cyst formation in the pancreatic head (arrow). (b) After corticosteroid therapy, the cyst formation markedly shrank.

Fig. (13). CT findings of focal AIP in a 79-year-old man.
(a) Reconstructed coronal image of early phase of dynamic contrast-enhanced CT shows a round, poorly enhanced area in the pancreas head (white arrow). (b) The lesion is homogeneously enhanced on delayed-phase contrast-enhanced CT image (white arrowheads).

Fig. (14). CT findings of pancreatic cancer in a 75-year-old man.
(a) Early phase of dynamic contrast-enhanced CT shows a poorly enhanced mass lesion in the pancreas body. (b) On delayed phase, the pancreas body lesion is heterogeneously enhanced, slightly enhanced in the margin (arrows) and poorly enhanced in the center (arrowhead).

Fig. (15). Dynamic contrast-enhanced MR findings of focal AIP in a 79-year-old man

(same case as in Fig. 13).
(a) Fat-suppressed T1-weighted image shows speckled hyperintense areas (white arrows). (b) On the early phase of dynamic MRI, speckled areas are well enhanced (white arrowheads). (c) On the delayed phase of dynamic MRI, the lesion is seen as a homogeneous area. (d) Photomicrograph of a low-power field reveals that speckled hyperintense areas correspond to residual pancreatic lobules (open arrows). B, common bile duct; D, duodenum.

Fig. (16). Case presentation 1
(a) Abdominal ultrasound shows a hypoechoic mass in the pancreas body (white arrow). (b) Reconstructed curved coronal image of early phase of dynamic contrast-enhanced CT shows a poorly enhanced lesion (white open arrow) in the pancreas. (c – d) Another slice of CT images shows bronchial thickening of the lung (white long arrows in c), hilar lymph adenopathy (white curved arrows in d). (e, f) Coronal image of contrast-enhanced CT shows bilateral renal lesions (dotted white arrows in e), paravertebral mass (white arrowhead in e), parasacral mass (arrow in e), right orbital mass lesions (white small arrow in f) and infraorbital nerve swelling (white arrowheads in f).

Fig. (17). Case presentation 2
(a) Early phase of dynamic CT shows the pancreas body and tail without abnormal lesion. (b) Coronal image of contrast-enhanced CT shows soft tissue density around the aorta (white arrows). (c) CT image 34 months after corticosteroid therapy shows a new pancreatic lesion with a capsule-like rim (small white arrows).

Fig. (18). Lachrymal and salivary gland lesions in a 50-year-old man.
(a) Ga-67 scintigram shows increased uptake in the bilateral lachrymal (arrows) and mandibular glands (arrowheads). (b) T2-weighted coronal image shows homogeneous swelling of the bilateral submandibular glands (white open arrows). (c) On a T2-weighted image of another coronal slice, homogeneous swelling of the bilateral lachrymal glands is seen (white thin arrows).

Fig. (19). Hilar lymph node adenopathy in a 68-year-old woman.

(a) Contrast-enhanced CT shows bilateral lymphadenopathy (white thin arrows). (b) Ga-67 scintigram shows increased uptake in the bilateral lachrymal (arrows) and submandibular gland (arrowheads) as well as hilum (open arrows).

Fig. (20). Various types of lung lesions.
(a – c) Thin-sliced CT shows a nodular lesion (white arrow in a), interlobular septal thickening (white small arrows in b) and consolidation (open arrows in c). Bronchial wall thickening is shown in Fig. **6e**.

Fig. (21). Bile duct lesion in a 77-year-old man.
(a) Axial T2-weighted image shows prominent wall thickening of the common bile duct (white arrow). (b) On a coronal-oblique T2-weighted image, intra-hepatic bile duct dilatation is mild, though extensive wall thickening of the common bile duct is seen.

Fig. (22). Peri-pancreatic lymphadenopahy in a 55-year-old man.
(a) Contrast-enhanced CT of the cranial side to the pancreas shows a paravertebral soft-tissue mass (open arrow) as well as multiple lymphnode swelling (arrows). (b) Three months after corticosteroid therapy, the lymphadenopathies are improved.

Fig. (23). Various types of renal lesions.
(a – c) Early phase of dynamic contrast-enhanced CT shows multiple poorly enhanced lesions in wedged or nodular shapes (parenchymal lesions) (a), soft-tissue density mass of the renal hilum (hilar lesion) (b) and perirenal soft-tissue density area (perirenal lesion) (c).

Fig. (24). Various types of retroperitoneal lesions.
(a -c) Contrast-enhanced CT shows para-aortic soft-tissue density (para-aortic type, white arrows in a), soft-tissue mass around the left ureter (periureteric type, white long arrows in b) and soft-tissue mass behind the pancreas (increased fat density type, white open arrows in c). Parabone-type lesions are shown in Fig. **16e** and Fig. **22a**.

Fig. (25). Pituitary lesion in a 55-year-old man (same case as in Fig. **22** and **23c**).
(a) Sagittal image of contrast-enhanced T1-weighted image shows swelling of the

pituitary gland and stalk (white arrows). (b) Pituitary abnormality is improved one month after corticosteroid therapy.

Fig. (26). Prostatic lesion in a 72-year-old man.
(a) Axial T2-weighted image shows swelling of the prostate. (b) On diffusion-weighted image, a diffuse hyperintense area is seen.

Fig. (27). Pericardial lesion in a 68-year-old man.
Contrast-enhanced CT shows diffuse pericardial thickening (white arrows), periaortic soft-tissue density (white arrowhead) and a paravertebral soft-tissue density (open arrow).

Fig. (28). *Ligamentum teres* lesion in a 50-year-old man (same case as in Figs. **16** and **23b**).
Contrast-enhanced CT shows poorly enhanced mass lesion of the *ligamentum teres* (white arrow).

Fig. (29). Multiple IgG4-related lesions without pancreatic lesions in a 65-year-old man.
(a) Fat-suppressed T1-weighted image shows that the signal of the pancreas is normal. (b) Coronal T2-weighted image shows bilateral submandibular gland swelling (white arrows). (c -e) CT image shows a nodular lesion in the lung (white long arrow in c), a paravertebral mass lesion (white open arrow in d) and a left renal lesion (white arrowhead in e). (f) The prostate is seen as a diffuse hyperintense area on diffusion-weighted image.

Fig. 1

Fig. 2a

Fig. 2b

Fig. 2c

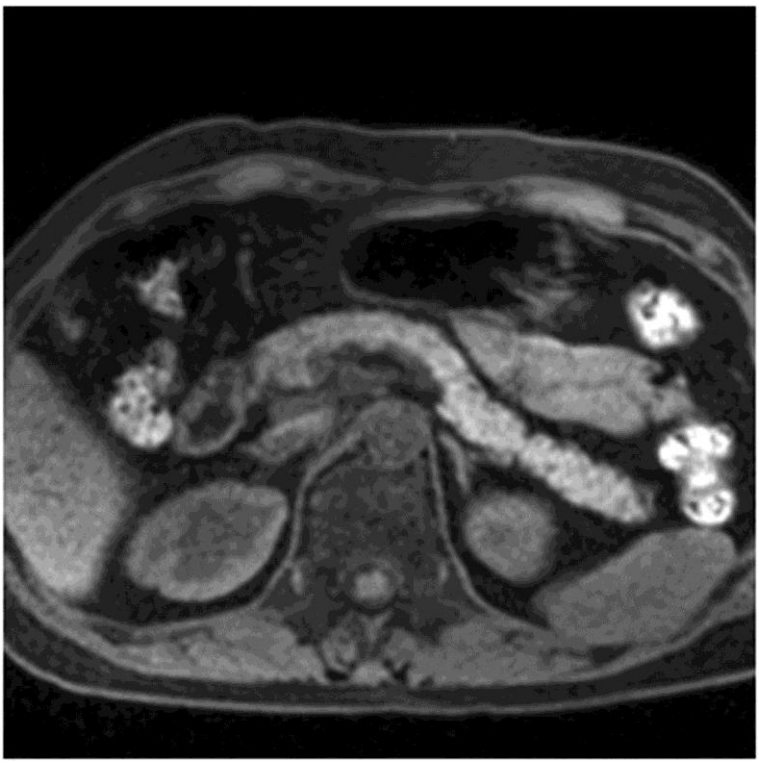

Fig. 3

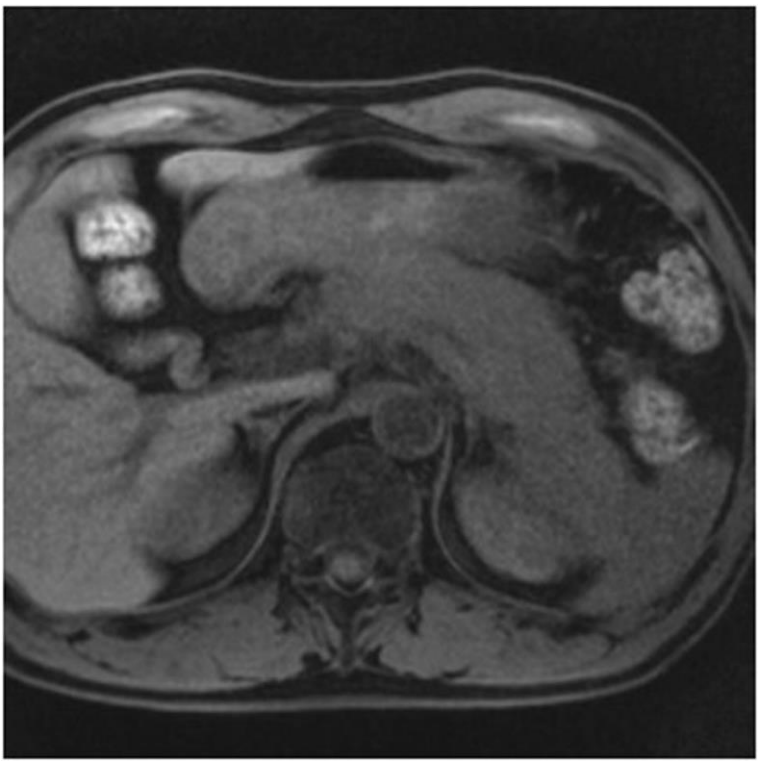

Fig. 4a

Fig. 4b

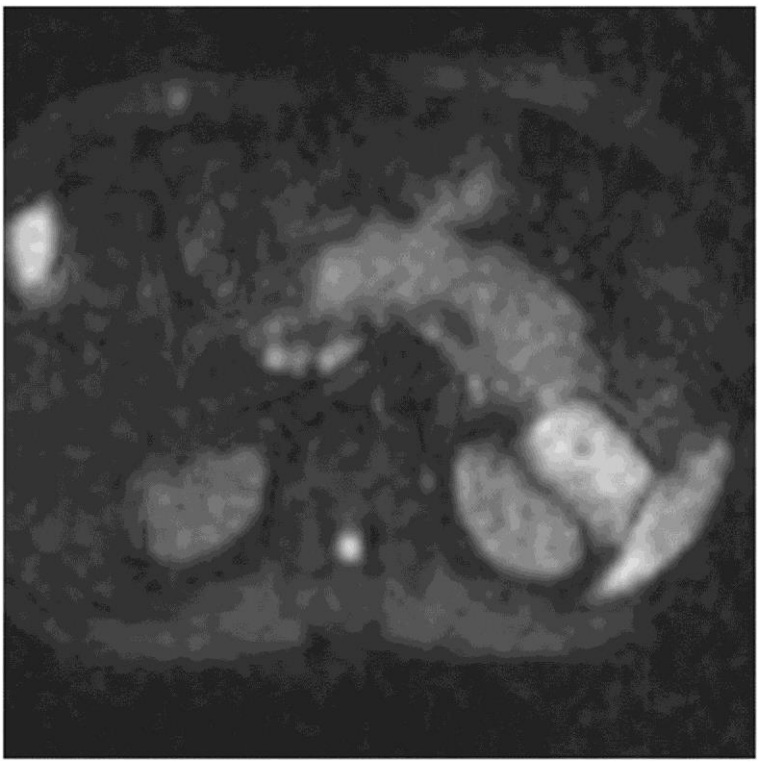

Fig.4c

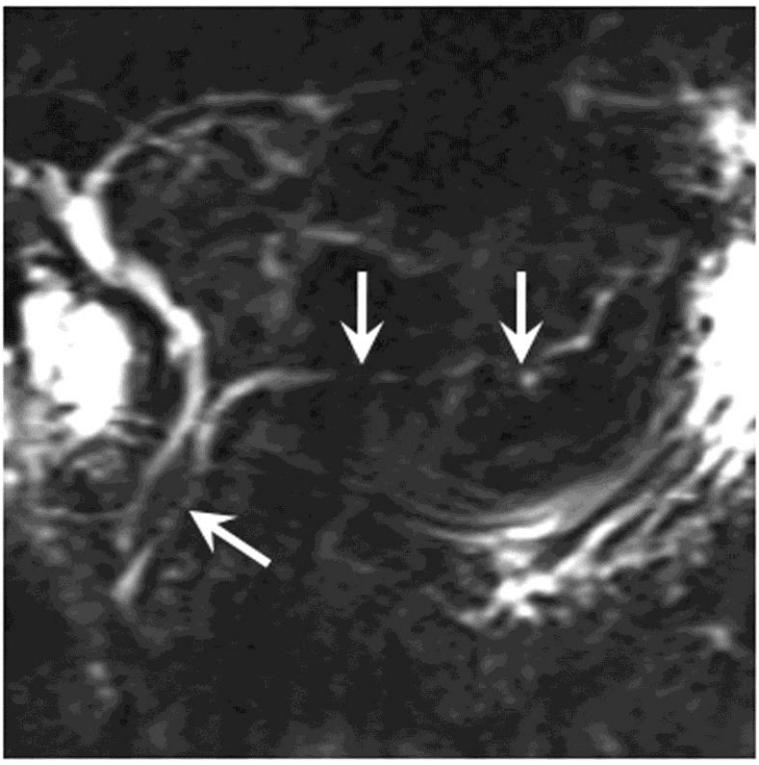

Fig. 5

Fig. 6a

Fig. 6b

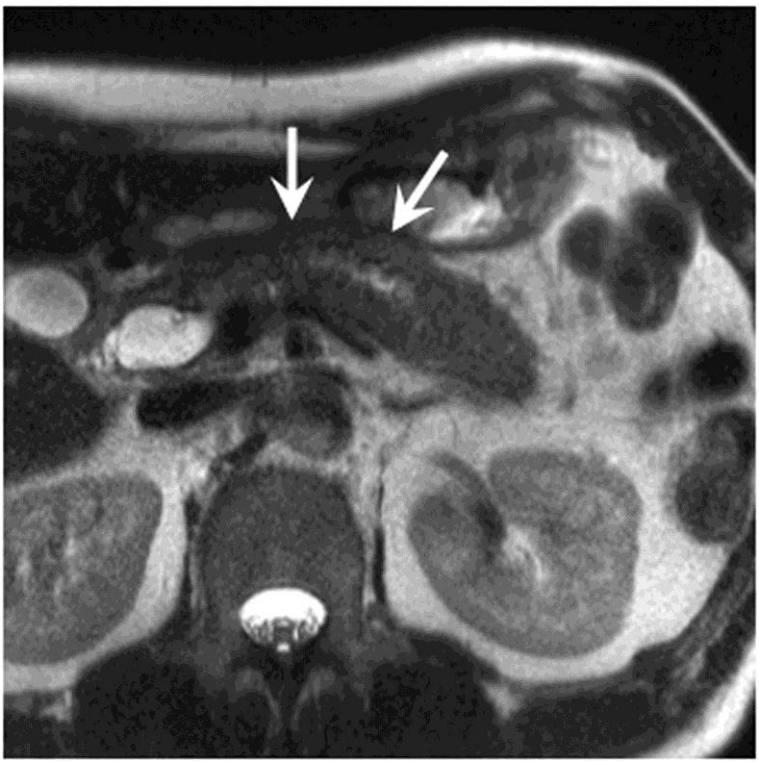

Fig. 6c

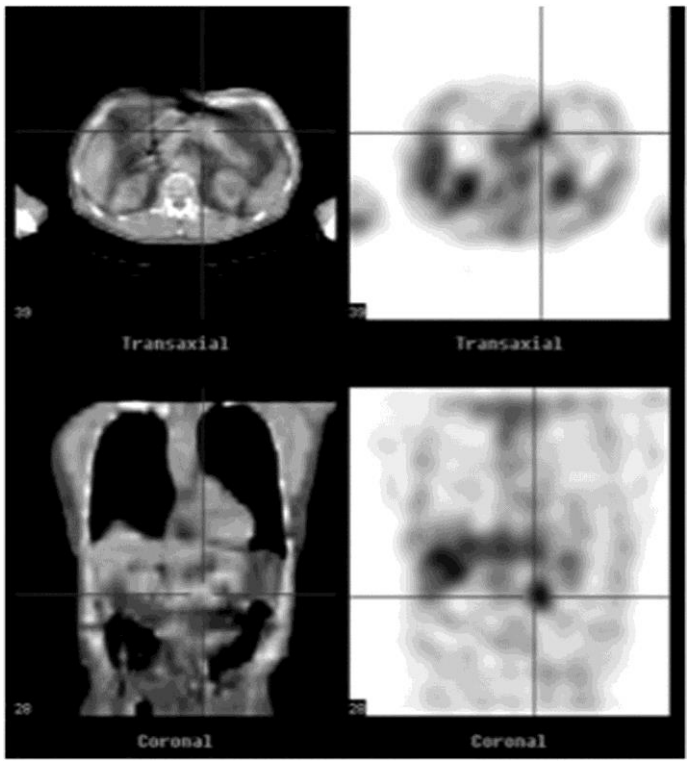

Fig. 7

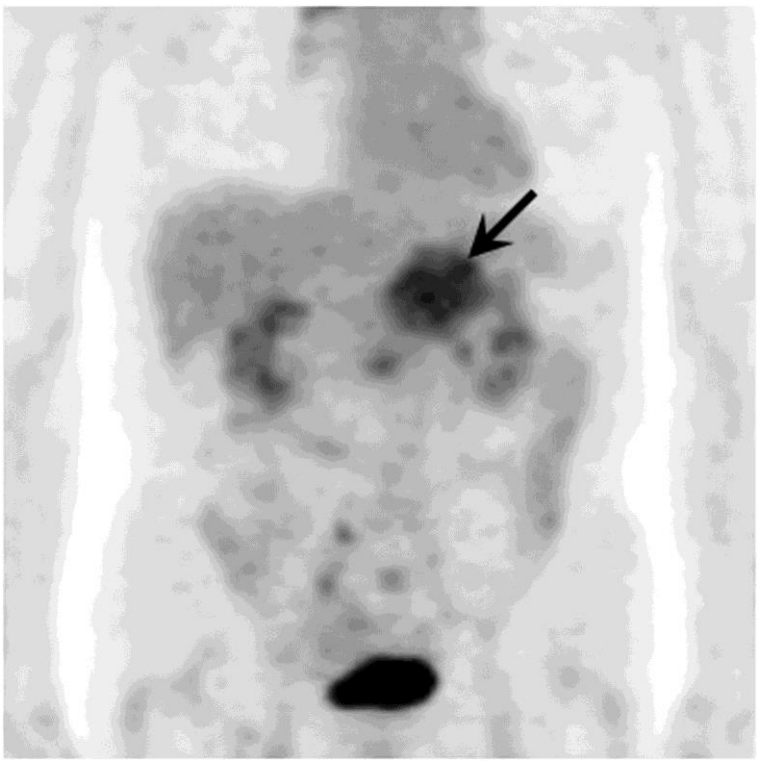

Fig. 8

Fig. 9

Fig. 10

Fig. 11

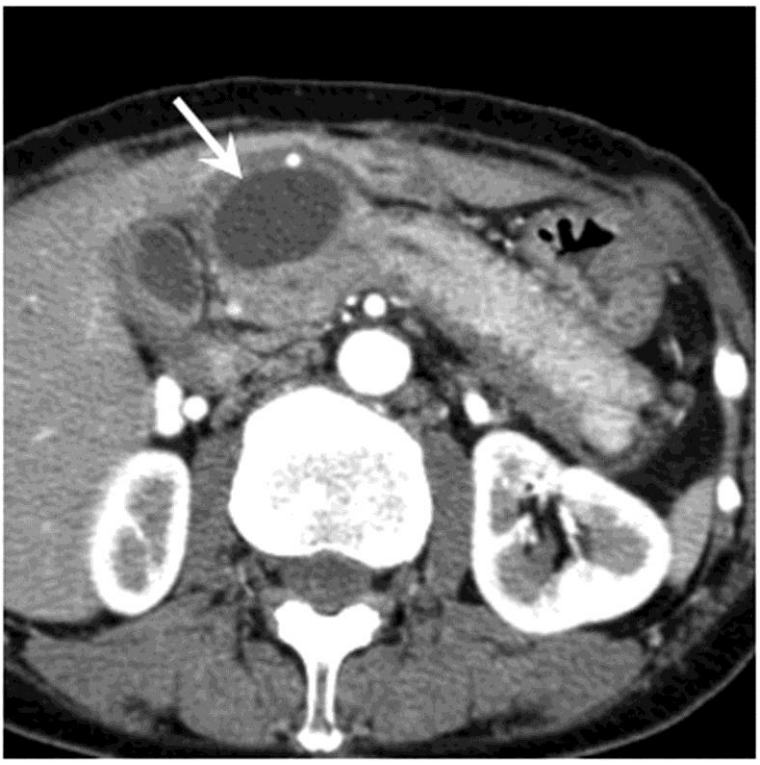

Fig. 12a

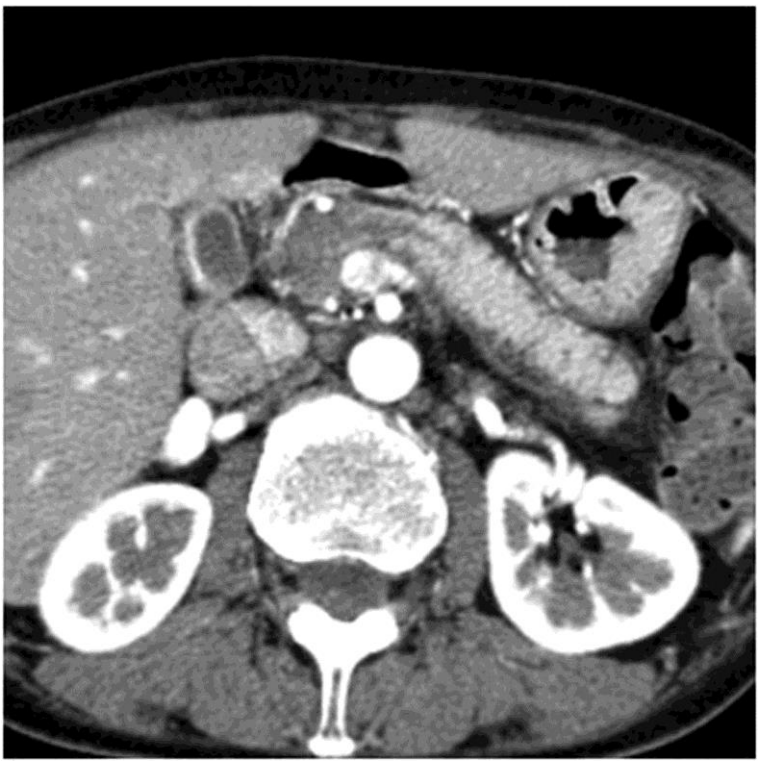

Fig.12b

Fig. 13a

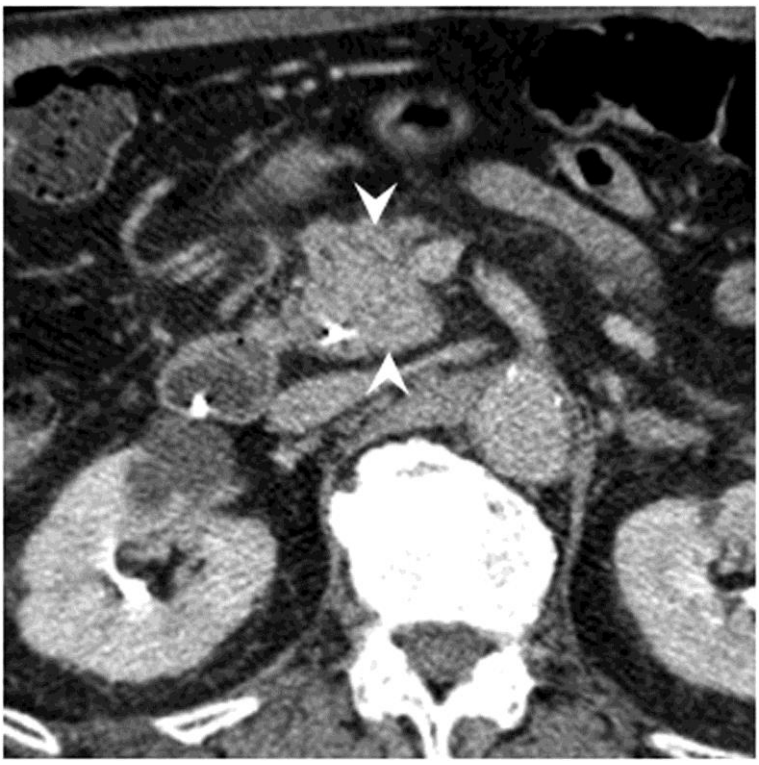

Fig. 13b

Fig. 14a

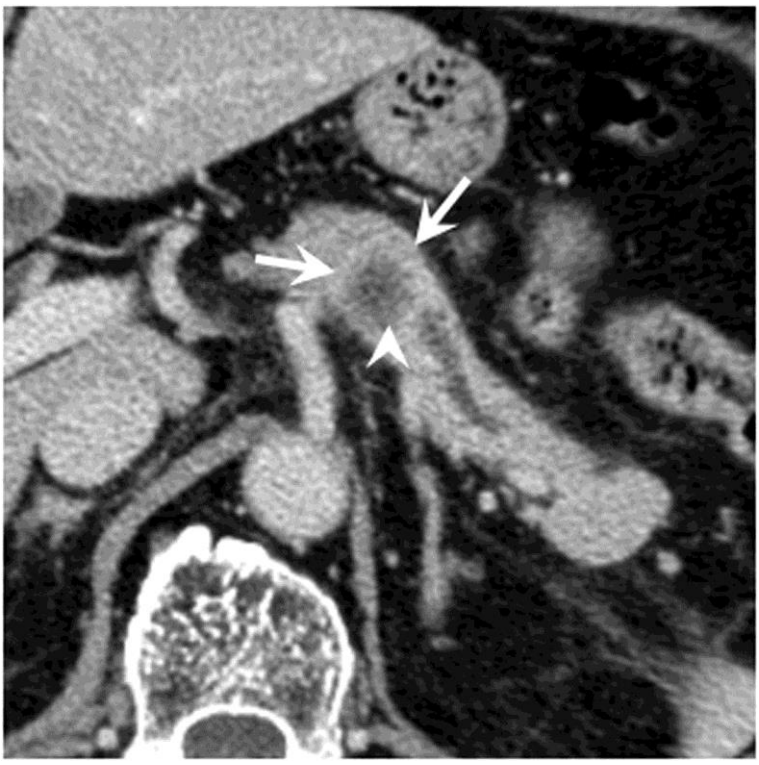

Fig. 14b

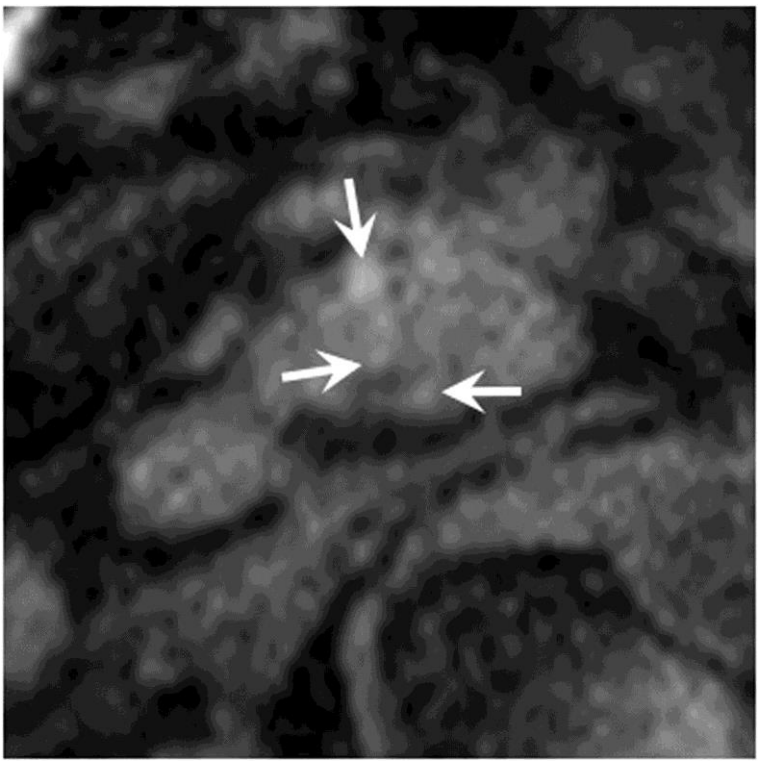

Fig. 15a

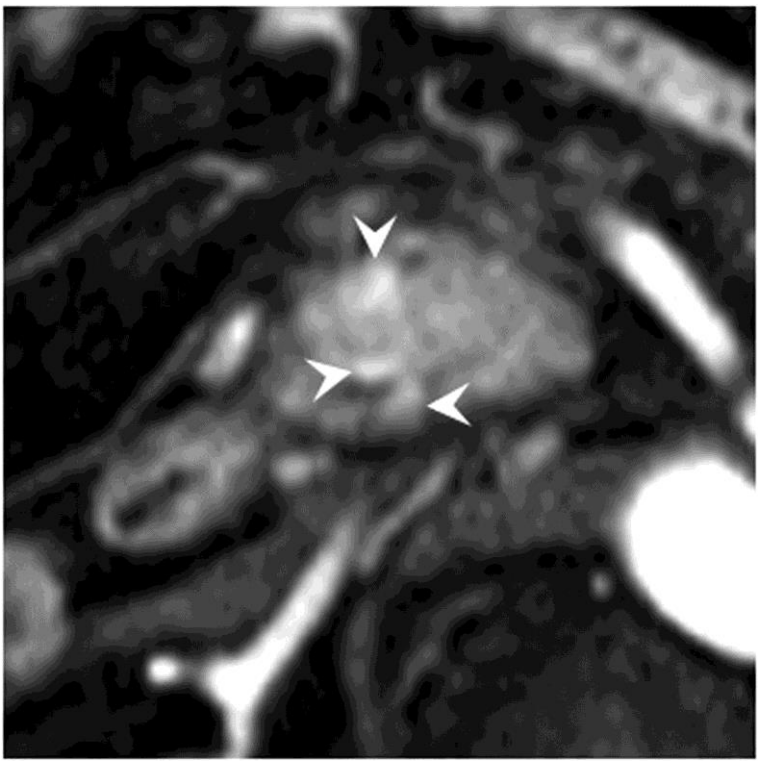

Fig. 15b

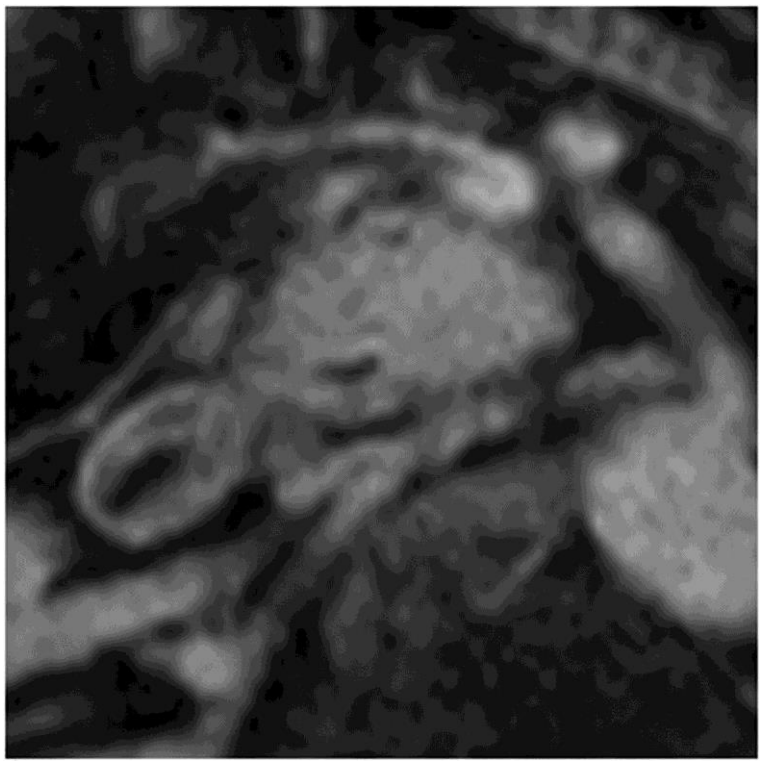

Fig. 15c

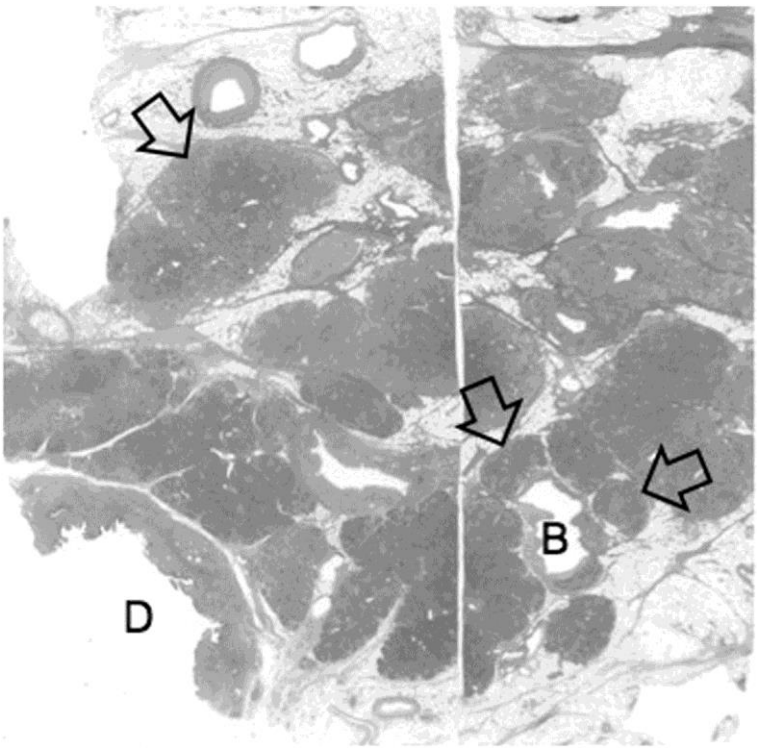

Fig. 15d

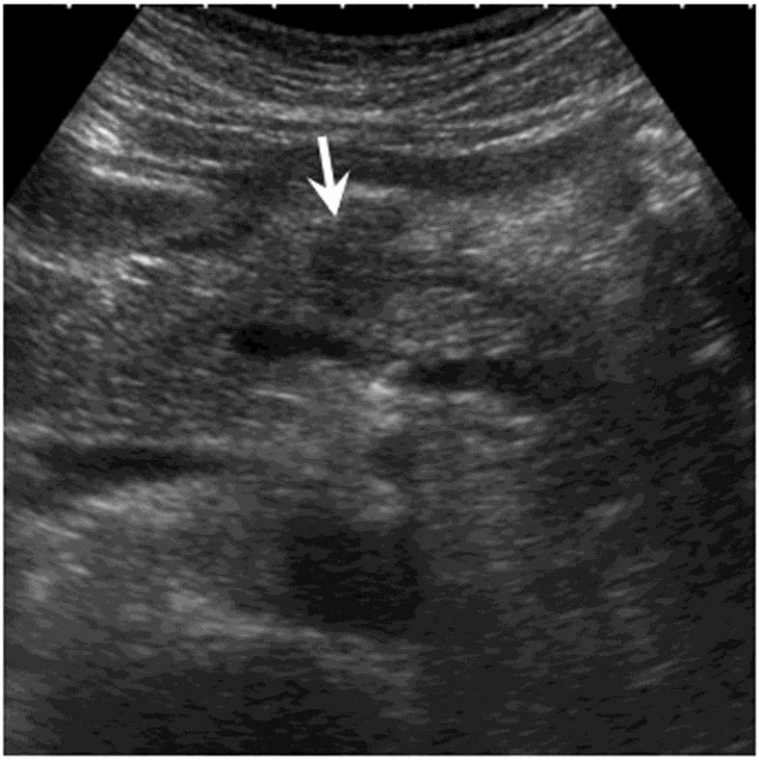

Fig. 16a

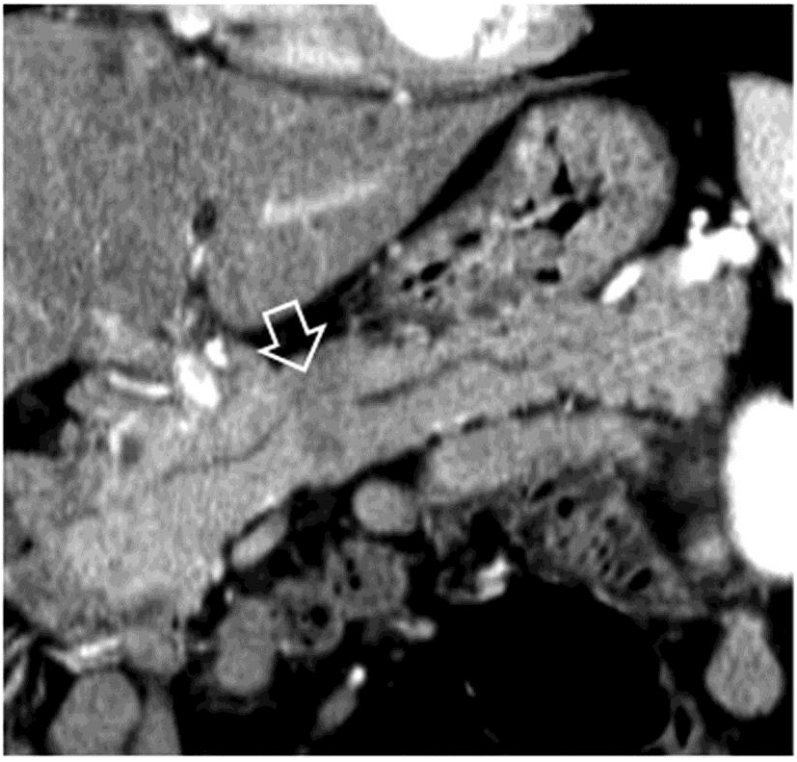

Fig. 16b

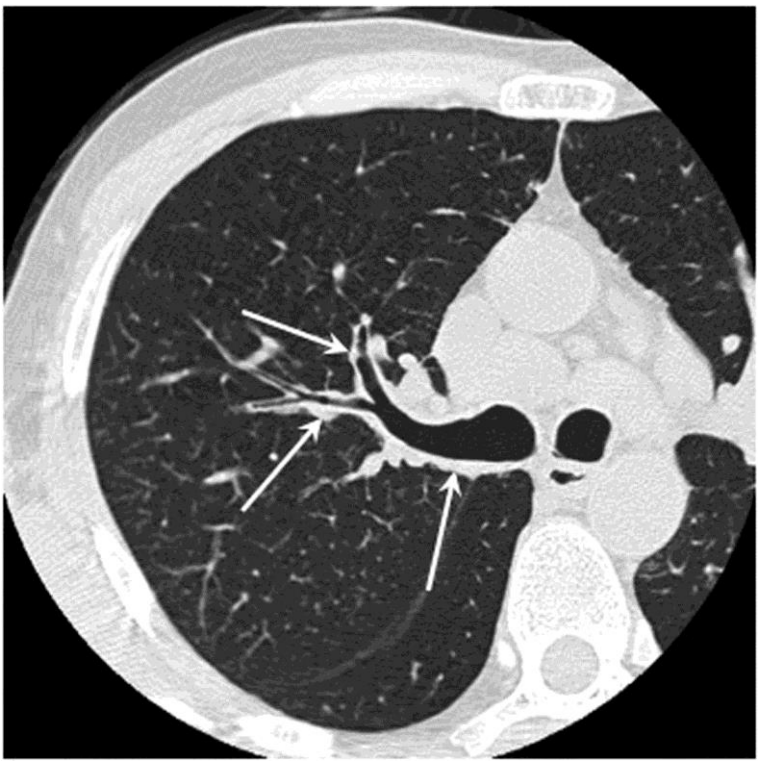

Fig. 16c

Fig. 17a

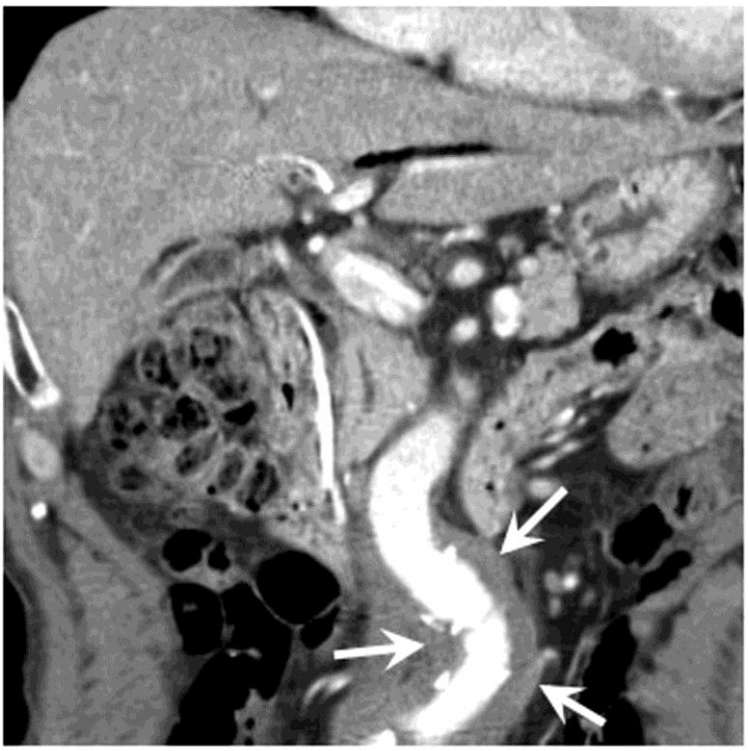

Fig. 17b

Fig. 17c

Fig. 18a

Fig. 18b

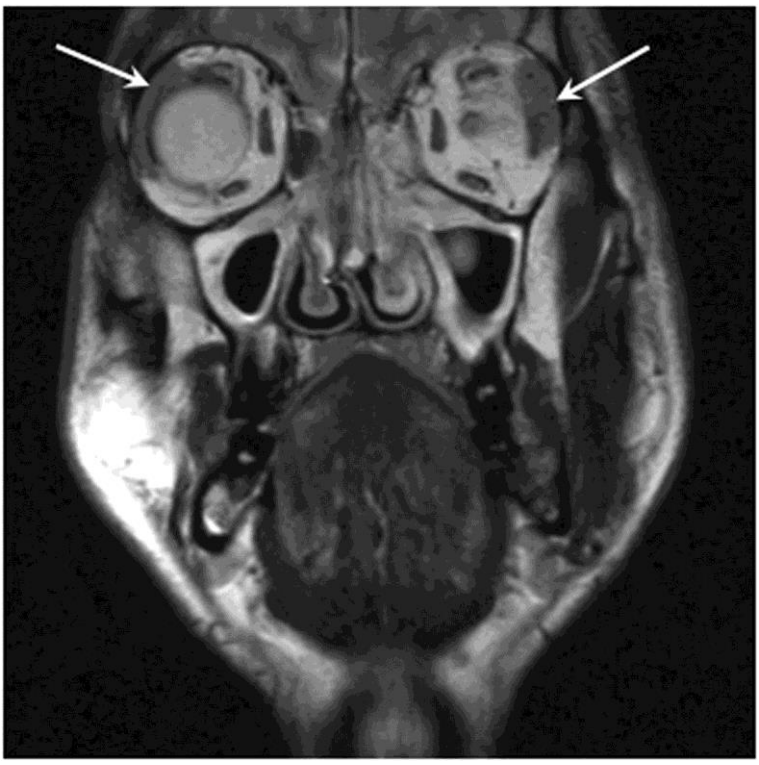

Fig. 18c

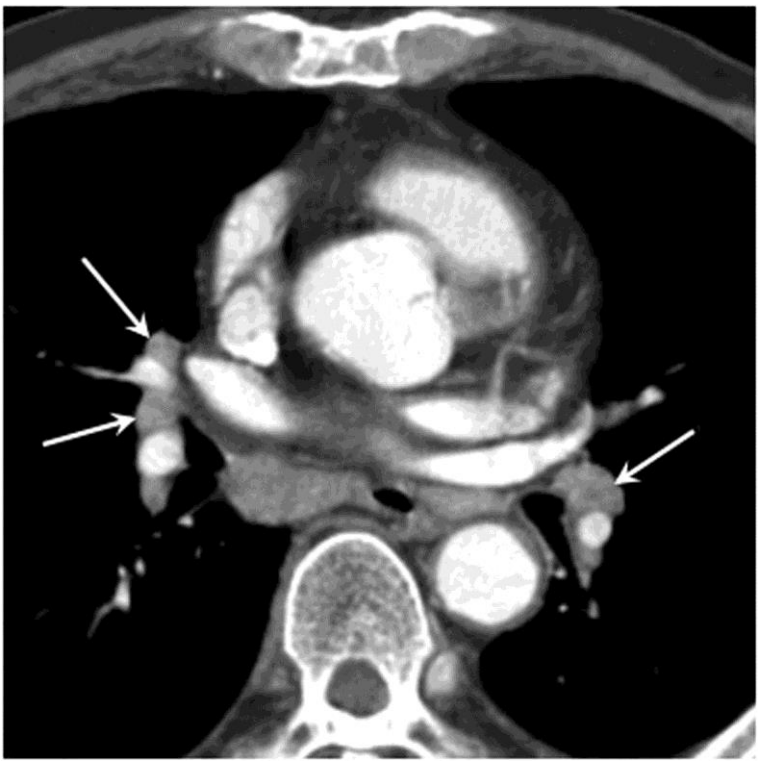

Fig. 19a

Fig. 19b

Fig. 20a

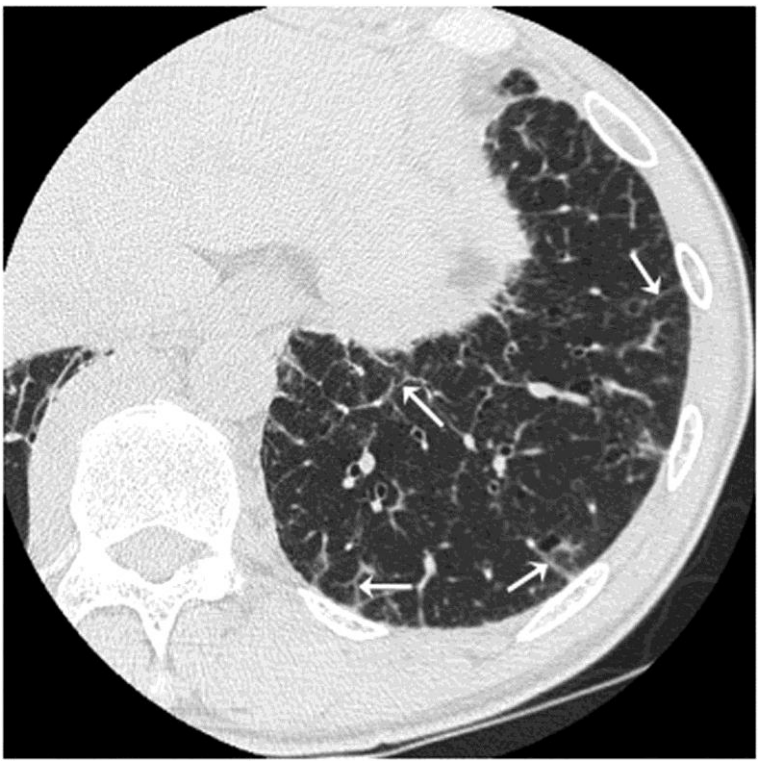

Fig. 20b

Fig. 20c

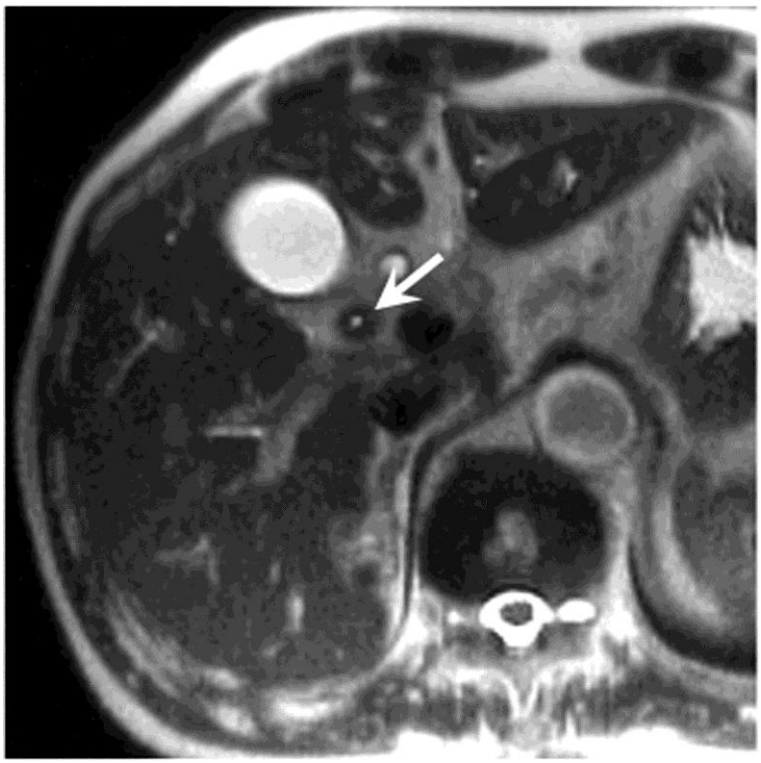

Fig. 21a

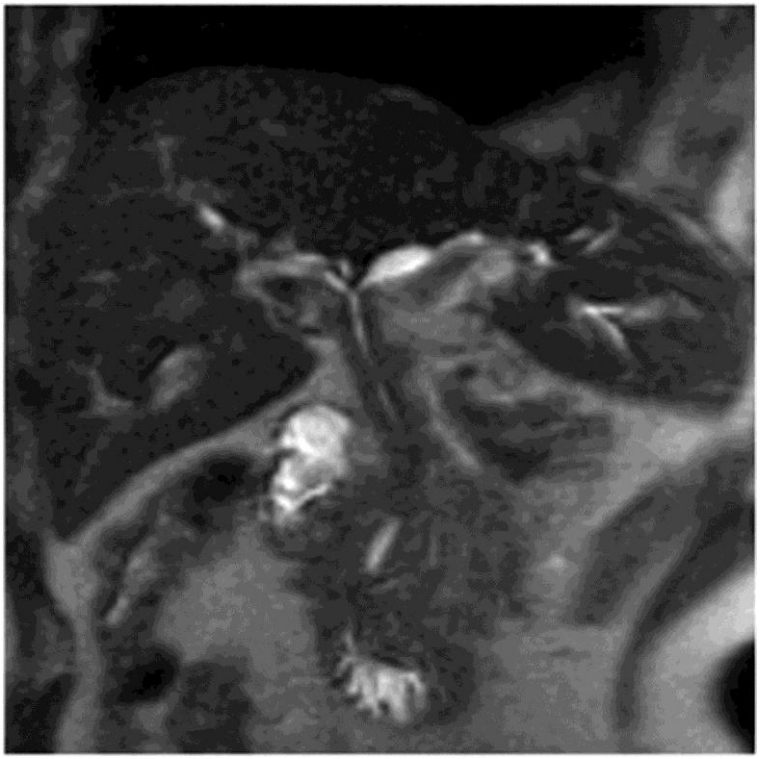

Fig. 21b

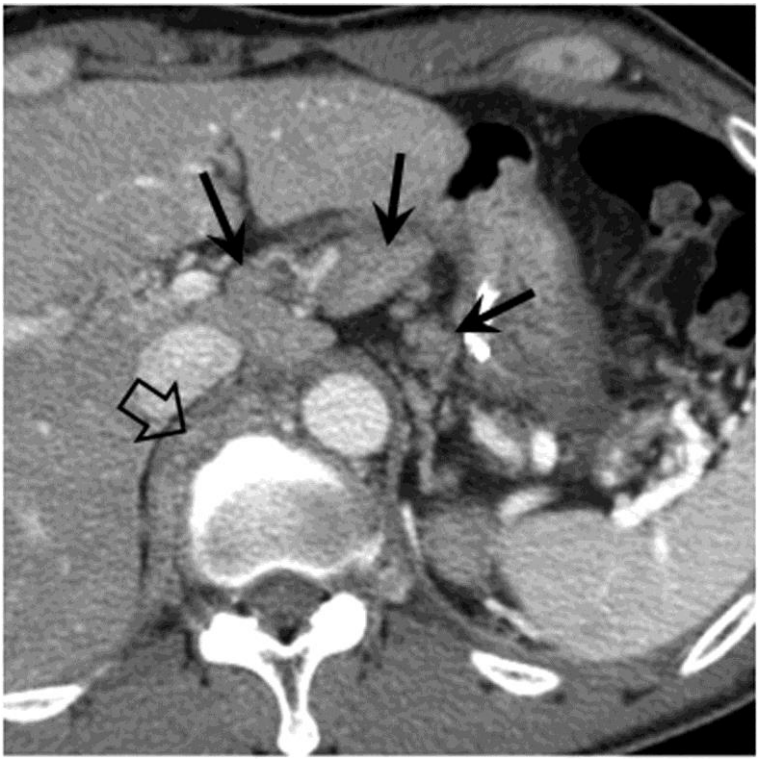

Fig. 22a

Fig. 22b

Fig. 23a

Fig. 23b

Fig. 23c

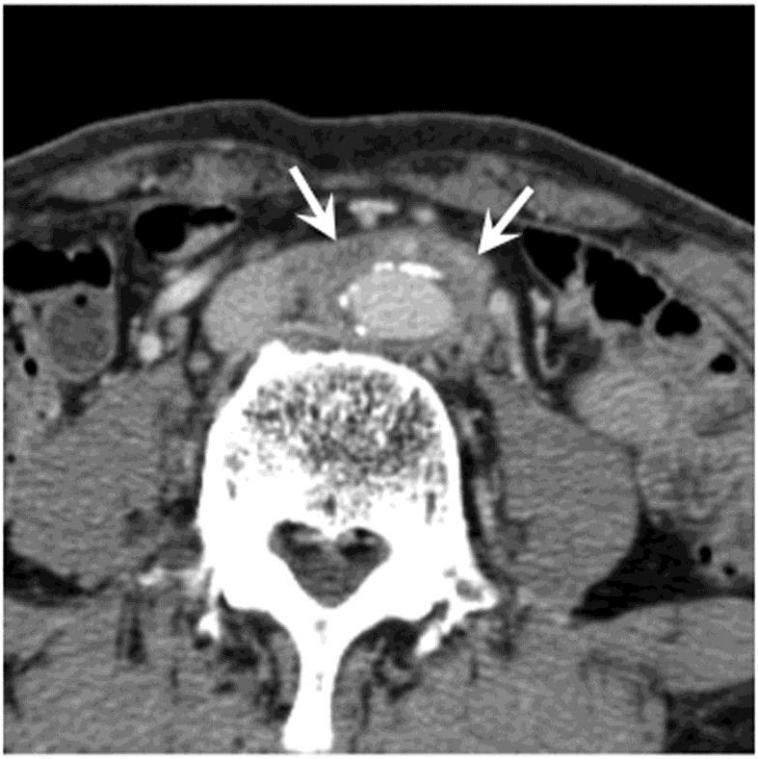

Fig. 24a

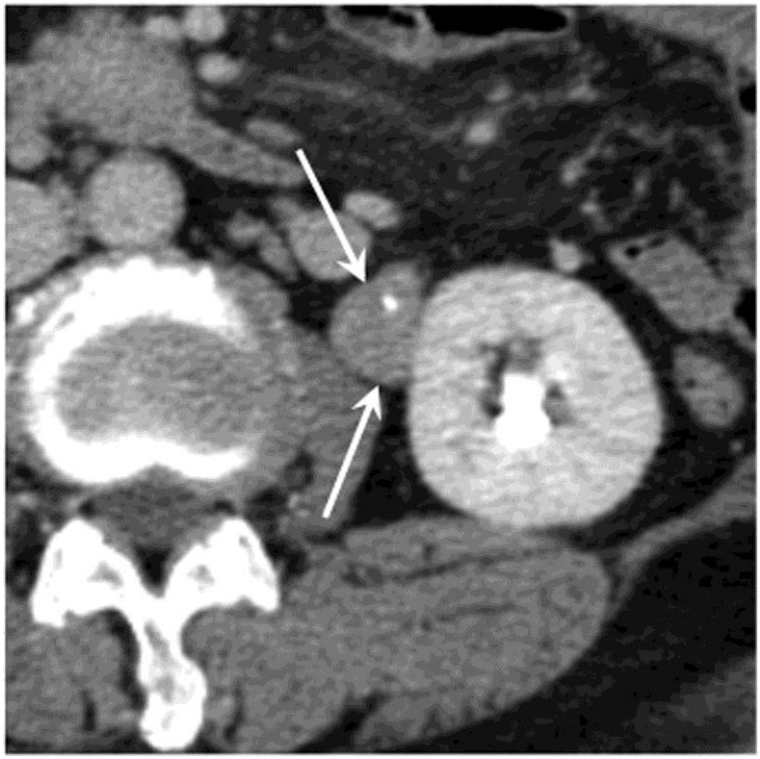

Fig. 24b

Fig. 24c

Fig. 25a

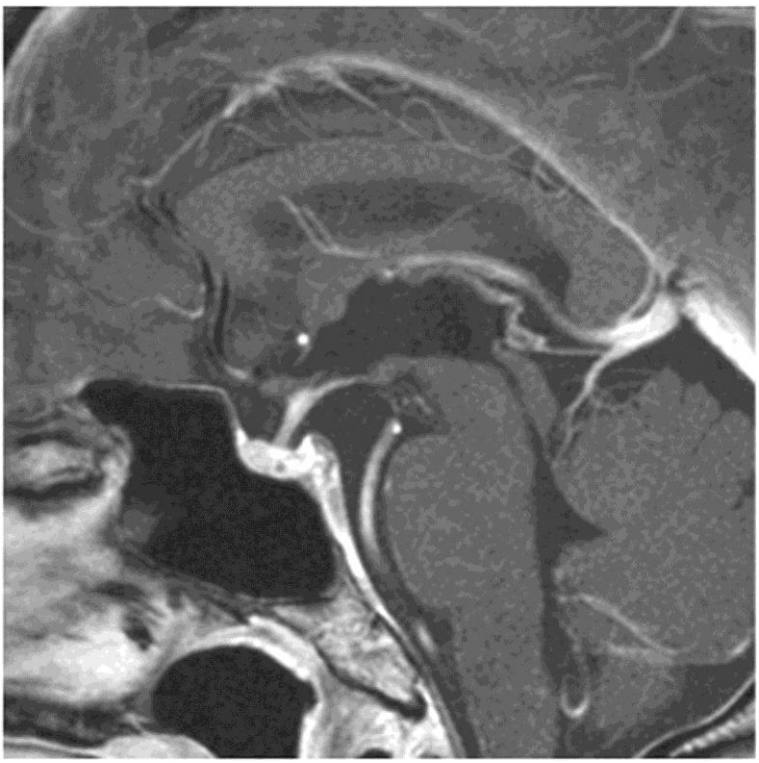

Fig. 25b

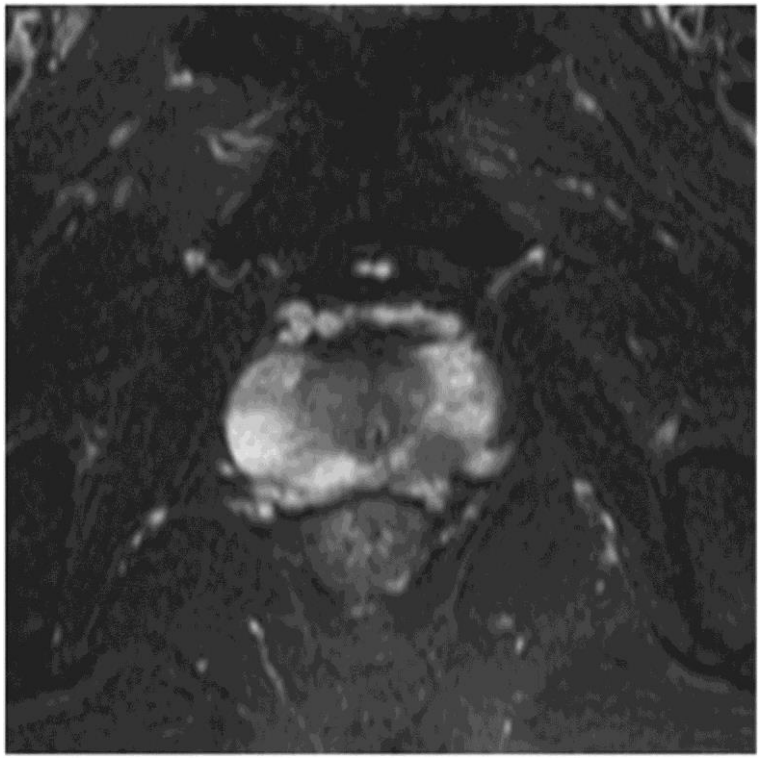

Fig. 26a

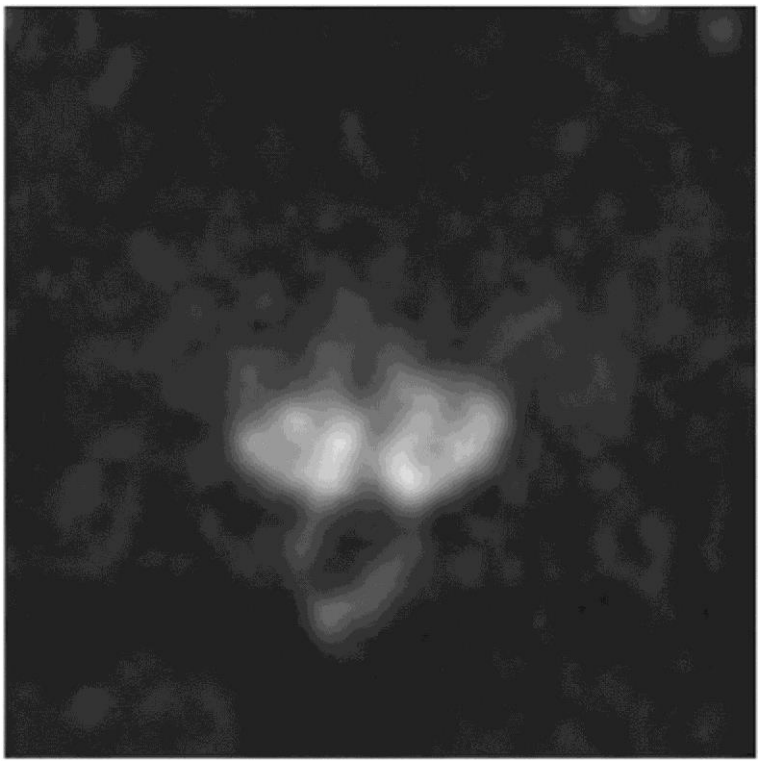

Fig. 26b

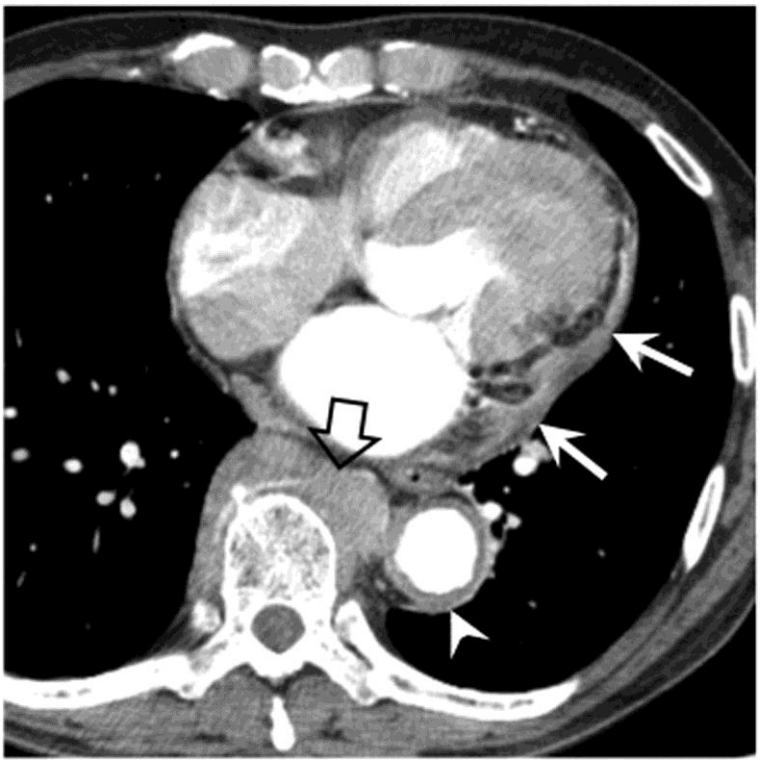

Fig. 27

Fig. 28

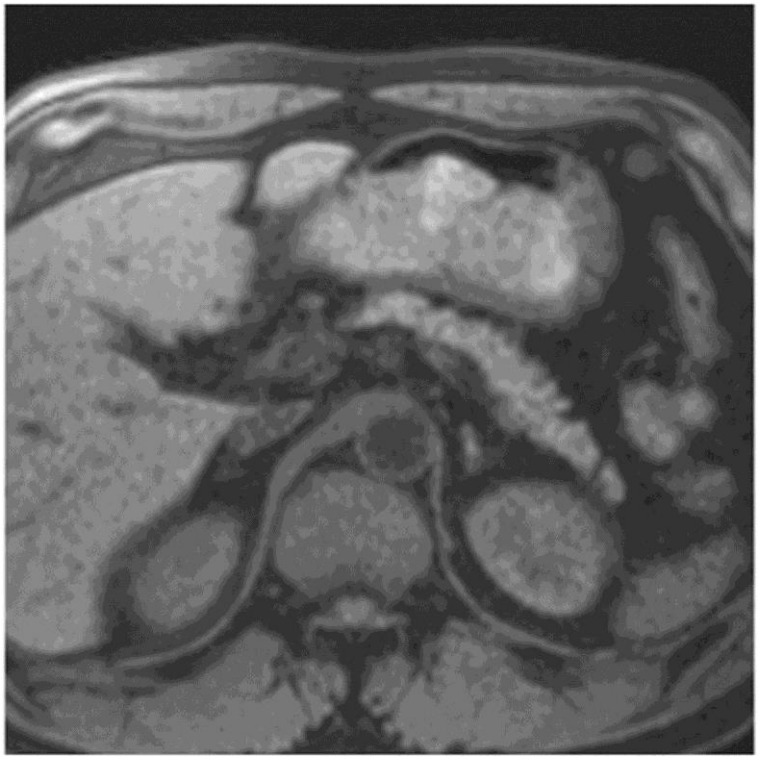

Fig. 29a

Fig. 29b

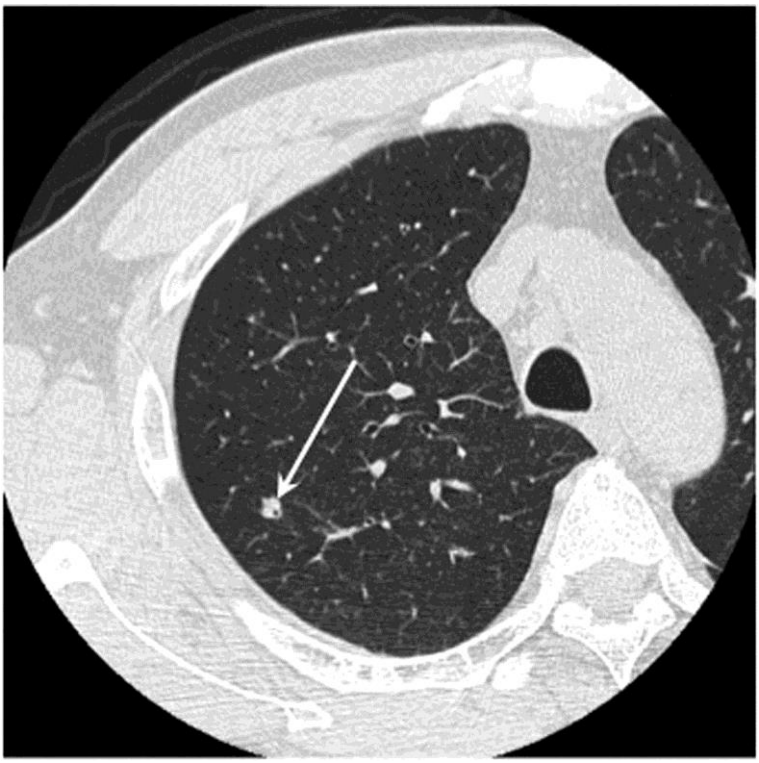

Fig. 29c

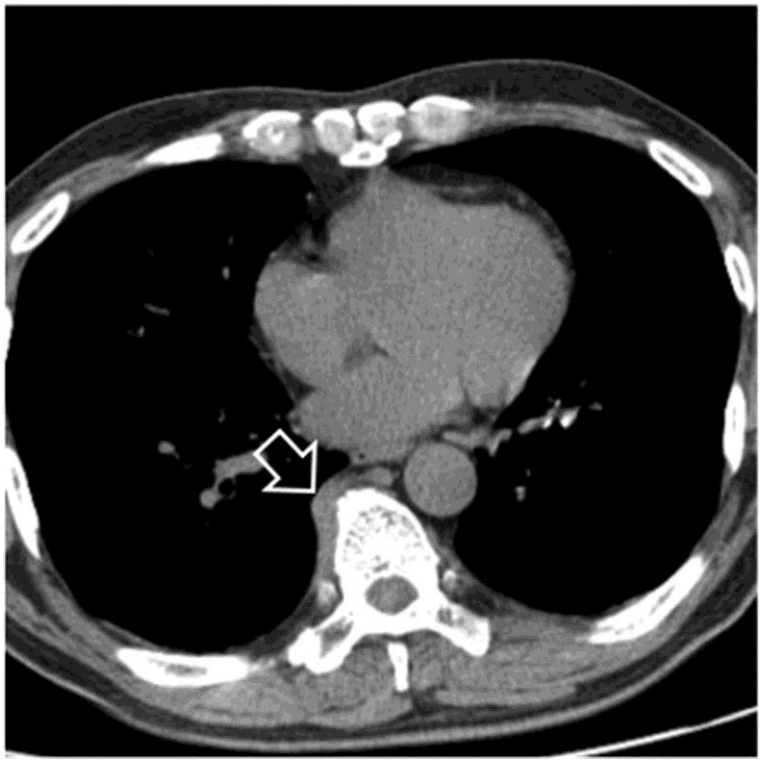

Fig. 29d

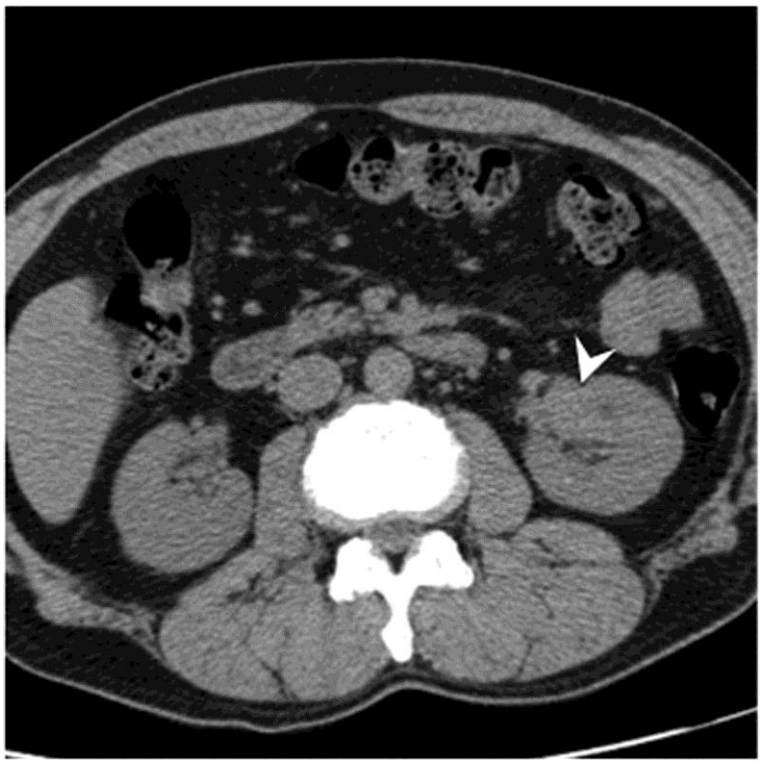

Fig. 29e

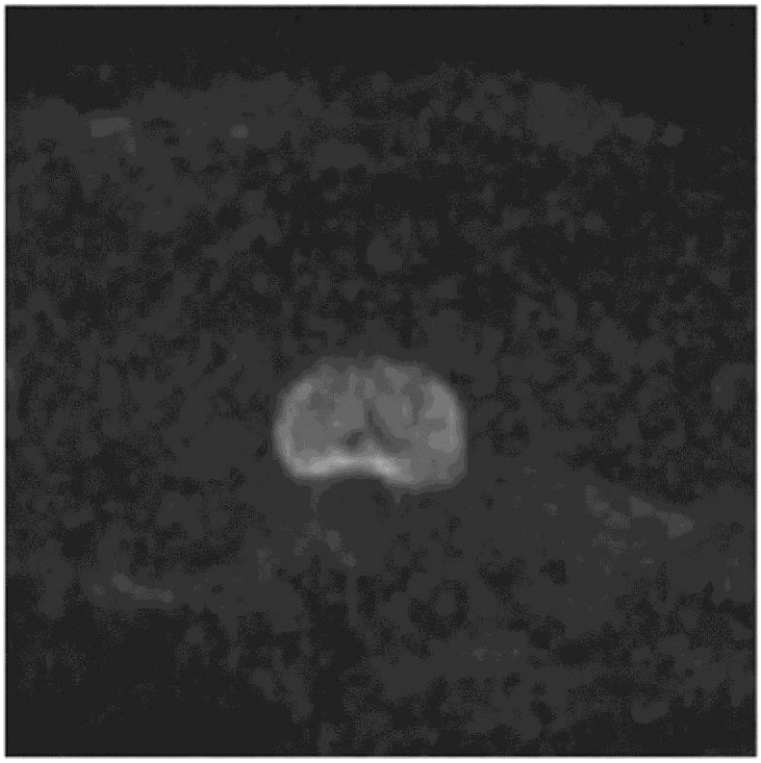

Fig. 29f